



Experimental study of foaming agents in water and their application in the metal foaming.

Master Thesis

Study programme:

N2301 Mechanical Engineering

Study branch:

Machines and Equipment Design

Author:

Mohammad Yousef Hdaib

Thesis Supervisors:

prof. Ing. Karel Fraňa, Ph.D.

Department of Power Engineering Equipment





Master Thesis Assignment Form

Experimental study of foaming agents in water and their application in the metal foaming.

Name and surname: **Mohammad Yousef Hdaib**
Identification number: S18000209
Study programme: N2301 Mechanical Engineering
Study branch: Machines and Equipment Design
Assigning department: Department of Power Engineering Equipment
Academic year: **2019/2020**

Rules for Elaboration:

1. Introduction to foaming process – effects of the additive materials on the foaming, comparison between metal and water-ethanol mixture.
2. The experimental analysis when fluid properties are changed like surface tension and viscosity, by adding foaming agents like Ethanol and Isopropyl alcohol in a way to imitate the process of adding additives to molten metal.
3. To calibrate it's viscosity and surface tension, and checking if there's a direct correlation between both of them.
4. Investigation of the multi-phase flow phenomena with and without magnetic fields, effects on the bubble and foam formation.
5. Analysis of experimental results, measurements using speed camera.
6. Quality evaluation of foams, effects of the bubble formation on the quality of foams.

Rozsah grafických prací:
Rozsah pracovní zprávy:
Forma zpracování práce:
Jazyk práce:

–
60 stran
tištěná/elektronická
Angličtina



Seznam odborné literatury:

1. J. J. Bikerman, Foams, Springer, 978-3-642-86736-1, 1973.
2. Henry Z. Kister, Distillation Operation, McGraw Hill Professional, 007034910X, 9780070349100, 1990
3. Nihad Dukhan, Metal Foams: Fundamentals and Applications, DEStech Publications, 978-1-60595-014-3, 2013.
4. John Banhart, , characterisation and application of cellular metals and metal foams, Pergamon, Volume 46, Issue 6 of Progress in materials science, ISSN: 0079-6425, 2001.

Vedoucí práce:

prof. Ing. Karel Fraňa, Ph.D.
Katedra energetických zařízení

Datum zadání práce:

1. listopadu 2019

Předpokládaný termín odevzdání: 30. dubna 2021

prof. Dr. Ing. Petr Lenfeld
děkan



doc. Ing. Petra Dančová, Ph.D.
vedoucí katedry

V Liberci dne 14. února 2020

Declaration

I hereby certify, I, myself, have written my master thesis as an original and primary work using the literature listed below and consulting it with my thesis supervisor and my thesis counsellor.

I acknowledge that my bachelor master thesis is fully governed by Act No. 121/2000 Coll., the Copyright Act, in particular Article 60 – School Work.

I acknowledge that the Technical University of Liberec does not infringe my copyrights by using my master thesis for internal purposes of the Technical University of Liberec.

I am aware of my obligation to inform the Technical University of Liberec on having used or granted license to use the results of my master thesis; in such a case the Technical University of Liberec may require reimbursement of the costs incurred for creating the result up to their actual amount.

At the same time, I honestly declare that the text of the printed version of my master thesis is identical with the text of the electronic version uploaded into the IS/STAG.

I acknowledge that the Technical University of Liberec will make my master thesis public in accordance with paragraph 47b of Act No. 111/1998 Coll., on Higher Education Institutions and on Amendment to Other Acts (the Higher Education Act), as amended.

I am aware of the consequences which may under the Higher Education Act result from a breach of this declaration.

June 10, 2020

Mohammad Yousef Hdaib

Acknowledgement.

First and foremost, praises and thanks to the God, for His blessings on throughout my study. I am extremely grateful to my parents for their support and prayers.

I would like to express my deep and sincere gratitude to my supervisors Dr. Karel Frana and Eng. Shehab Attia. Also, I express my gratitude to the Department of power engineering equipment in TUL. Finally, thanks to all people who helped me out to finish this project successfully.

Mohammad Hdaib.

Abstract.

In this study an experimental investigation was performed on foaming process of water-alcoholic mixtures. The aim of this study is to provide an illustration on foaming phenomena in water alcoholic-mixtures, and an investigation of its application in foaming process in molten metal. In the first and second sections of this study a comprehensive review was presented on physiochemical properties and theory of foaming process in both water-alcoholic mixtures and molten metal. In the third and fourth parts a description of the experimental setup and procedures were presented with results. In the last section a conclusion of results was presented. The used experiment has three main parts: in the first part best foaming conditions were specified by air injection in water-ethanol and water-isopropanol mixtures at different alcoholic volume fractions from 0 to 1 at 50 L/h flow rate and 20 seconds foaming time. While in the second part foaming behavior analyzed at different flow rate (15, 25, 50 and 75 L/h) and foaming time (20, 35, 55 seconds). In the third part, drainage velocity was calculated by using a proposed method based on literature data. Furthermore, an Image processing code was written to analyze experimental data. According to previous measured data, the dimensionless parameters: Reynolds, Marangoni, and Capillary numbers were calculated. The result of this study shows that, for water-isopropyl mixtures foam did not appear, while for water-ethanol mixtures a best foaming condition occurred at 0.15 ethanol volume fraction. Also, the drainage velocity was mainly a function of foam thickness.

Keywords: foaming process, surface activity, Marangoni effect, Image processing, cross polarization, and surface tension.

Contents.

List of Figures.....	10
List of tables.....	11
List of symbols.....	12
1. Introduction.....	13
2. Theory.....	15
2.1. Physiochemical properties of molten Al-Si alloy.	15
2.1.1. Density.....	15
2.1.2. Viscosity.	15
2.1.3. Surface tension.	17
2.2. Physiochemical properties of water-alcoholic mixtures.	17
2.2.1. Density.....	18
2.2.2. Viscosity.	19
2.2.3. Surface tension.	20
2.3. Foaming process in molten metal.	21
2.3.1. Types of foaming processes in molten metal.	21
2.3.2. Effect of additives and foaming method on metal foam properties.	22
2.4. Foaming process in water-alcoholic mixtures.....	24
2.4.1. Viscosity and surface tension effect.	25

2.4.2. Magnetic field effect.....	25
2.4.3. Collapse time.	26
2.4.4. Drainage rate.....	26
2.4.5. Defoaming agents.	28
3. Experimental setup.....	29
3.1. Part one: Best foaming condition.	33
3.2. Part two: flow rate and foaming time effect.....	33
3.3. Part three: calculation of drainage velocity.....	34
3.4. Part four: similarities between foaming process in water-ethanol mixture and Al-Si alloy.	35
4. Results.....	36
4.1. Part one: Best foaming condition.	36
4.2. Part two: flow rate and foaming time effect.....	41
4.3. Part three: calculation of drainage velocity.....	49
4.4. Part four: similarities between foaming process in alcoholic mixture and Al-Si alloy.....	49
5. Conclusion.	51
5.1. Best foaming condition.	51
5.2. Effect of flow rate and foaming time on diameter and number of bubbles.	52
5.3. Drainage velocity and dimensionless numbers.	52

5.4. Similarities between foaming process in water alcoholic mixture and Al-Si alloy.	53
5.5. Magnetic field effect.	53
Bibliography	54
Annex 1: Image Processing Code.	58

List of Figures.

Figure 1: Density of Al-Si Alloy at different silicon molar fraction.15

Figure 2: Viscosity of Aluminum-Silicon alloy at different silicon molar fraction.
.....17

Figure 3: Surface Tension of Al-Si Alloy at different silicon molar fraction...17

Figure 4: Density (Kg/m³) of water+ethanol and water+2-Propanol mixtures[20], [26].18

Figure 5: Viscosity of water + ethanol and water + 2-Propanol mixtures [20], [26].
.....19

Figure 6: Surface Tension of water + ethanol and water + 2-Propanol mixtures [20],[22].20

Figure 7: Direct foaming method [27].22

Figure 8: Forces acting on bubble film.24

Figure 9: Experimental setup.29

Figure 10: Cross polarization effect. Images where taken by Huawei P9 lite camera and flashlight of Samsung S5 was used. a) unpolarized image, b) Polarized image.30

Figure 11: Comparison between measured data for isopropyl and ethanol mixtures.38

Figure 12: Foaming time and flow rate effect on number of bubbles.42

Figure 13: Foaming time and flow rate effect on diameter.42

List of tables.

Table 1: Viscosity according to Moelwyn-Hughes and Hirai models.....	16
Table 2: Properties of aluminum foam according to production method.	23
Table 3: Different types of additives used in the literature to stabilize aluminum foam.	23
Table 4: Dimensionless parameters which describe a bubble on liquid surface.	27
Table 5: Image preprocessing steps.	31
Table 6: Measured properties for water ethanol mixture.....	36
Table 7: Measured properties for water isopropyl mixture.	37
Table 8: Part one results.....	39
Table 9: Results of processed images for part 2.	41
Table 10: Part two results.	43
Table 11: Part three results: drainage rate and dimensionless parameters.....	49
Table 12: Similarities between foaming process in molten Al-Si and Water-ethanol.....	50

List of symbols.

Greek letters:

- ρ Density (kg/m^3).
- η Dynamic viscosity ($\text{mPa}\cdot\text{s}$).
- σ Surface tension (mN/s).
- Ω Dimensionless interaction parameter.
- θ Contact angle.

English letters:

- A, B Hirai model constants.
- Ca Capillary Number.
- D Diameter (mm).
- H Foam thickness (mm).
- L Lamella's length (mm).
- M Atomic mass.
- Mr Marangoni Number.
- N Number of bubbles.
- Q Volume.
- R Gas constant.
- r Radius (mm).
- Re Reynold's Number.
- T Temperature (K).
- t Time (s).
- U Drainage velocity (mm/s)
- V Volume fraction.
- X Molar fraction.

English subscripts:

- b Bubble.
- bo Border.
- c Curvature.
- E Ethanol.
- eff Effective.
- l Liquid.
- m Mixture.
- O Initial.
- P Isopropyl.
- T Total
- u Unit.
- W Water.

1. Introduction.

Foaming phenomena in general occurs in many industries and applications. Usually it is an unpleasant process for the most of chemical industries because it causes many problems such as flooding in distillation towers. Moreover, foam is hard to control when appears in several components during production process. On the other hand, foaming phenomena is preferable in some cases, such as production of metal foam. So that, scientific research regarding foaming process are crucially important.

In case of metal foam, the first patent for direct foaming process was provided for Jin et. al. [1] in 1990. After that, further investigations on foam stability were performed [2], [3], [4] and [5] investigated additives effects on foam stability and quality for different foaming processes in molten metal. In addition, many experimental studies were performed on molten metal properties. T.Lida et. al. [6] proposed one of the most cited studies for physiochemical properties of molten metal, at which they analyzed and compared physical properties of several liquid metals. Furthermore, R.Takaki et. al. [7] measured surface tension of molten aluminum, Nickel and iron as a function of temperature using oscillating droplet method and electromagnetic levitation. As well as, X. J. Han et. al. [8] used embedded atom method to calculate the density and specific heat of liquid Titanium and Aluminum alloys at temperatures above and below the melting temperature in a wide composition range. For this study properties of Al-Si alloy were used for comparison with water-alcoholic mixtures. Therefore, Moelwyn-Hughes model [9] and Hirai model [10] were used to predict viscosity of Al-Si alloy at different silicone volume fraction.

On the contrary, for Alcoholic mixtures Marangoni [11] analyzed relation between surface tension and bubbles lamellas thickness and Marangoni effect named after his name. Also, plateau [12] investigated relation between viscosity and foaminess. Afterwards research regard measurement of Marangoni effect performed by Lunkenheimer et. al. [13], A, Prins et. al. [14]. As well as, F, Schutz et. al. [15]

performed a study on foam stability using a closed glass storage by shaking it and calculating time for foam to be destroyed, they applied their study on several types of Alcohol included ethanol and isopropanol. On the other hand, Many studies focused on defoaming and anti-foaming agents [16], [17], [18], [16] and [19], which is not the main scope of this study.

This study focused on foaming process in alcoholic mixtures. Density and viscosity of aqueous ethanol and secondary propanol mixtures were measured at different alcoholic volume fractions and compared with literature results. Khattab et. al. [20] provided a temperature dependent numerical model based on experimental data for density, viscosity and surface tension for water ethanol mixture. Pang et. al. [21] performed experimental study on density and viscosity of aqueous primary and secondary propanol mixtures. Vazquez et. al. [22] performed surface tension study of different water alcoholic mixtures. The previous mentioned studies were compared with this study measured values. As shown in section (2.2.).

In this study there are two main sections: theoretical section, focuses on physiochemical properties of water alcoholic mixtures and molten Al-Si Alloy, as well as foaming process phenomena in both cases. While in the experimental section, experiment performed to investigate best foaming conditions and effects of flow rate and foaming time on foam structure, by using image processing techniques.

2. Theory.

2.1. Physiochemical properties of molten Al-Si alloy.

In this section the physiochemical properties of Al-Si Alloy were illustrated. The illustrated data are from literature. For density and surface tension, diagrams were written based on Schmitz et. al. [23] and Kobatake et. al. [24] studies. While for viscosity, Hirai and Moelwyn-Hughes models were used.

2.1.1. Density.

Figure (1), illustrates the density of Aluminum silicon alloy at different silicon molar fraction according to Schmitz et. al. [23] with linear data regression the last five points were calculated using regression equation of their results.

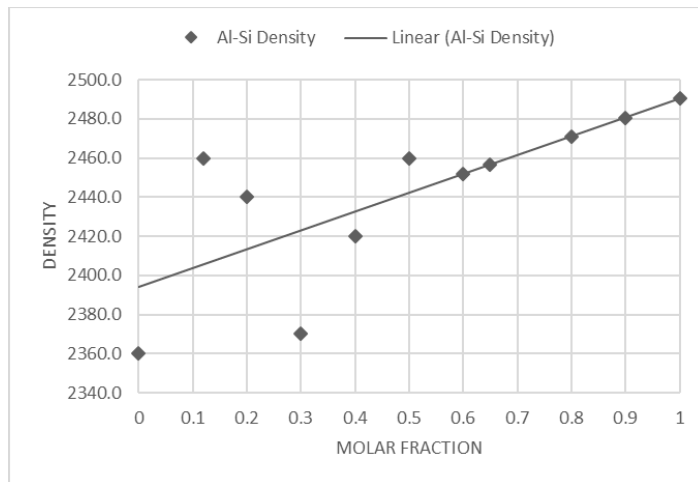


Figure 1: Density of Al-Si Alloy at different silicon molar fraction.

2.1.2. Viscosity.

For viscosity no one provided an experimental data at full range of Silicon molar fraction so that here is a calculation for Hirai and Moelwyn-Hughes models. Moelwyn-Hughes model [9] was used to find the viscosity of molten Al-Si at different silicon molar fraction, while Hirai model [10] is used to find the viscosity of pure Aluminum and Pure Silicon. Moelwyn-Hughes model is illustrated in

equation (1), where (x), (η), (Ω), (R) and (T) are molar fraction, Viscosity, dimensionless interaction parameter, gas constant and temperature, (A) and (B) subscripts indicate any arbitrary matters. In our case for Aluminum-Silicon alloy (Ω) equals to -2456 [25].

$$\eta = (x_A \eta_A + x_B \eta_B)(1 - 2x_A x_B \Omega / RT) \quad (1)$$

As shown in equation (2) Hirai Model was used to find viscosities of pure aluminum and pure Silicon. Where (T_m), (T) and (M) are Melting temperature, liquid metal temperature and atomic mass.

$$\eta = A \exp\left(\frac{B}{RT}\right) \quad (2)$$

$$B = 2.65 T_m^{1.27} \text{ (J.mol}^{-1}\text{)}$$

$$A = \frac{1.7 * 10^{-7} \rho^{\frac{2}{3}} T_m^{\frac{1}{2}} M^{-\frac{1}{6}}}{\exp\left(\frac{B}{RT_m}\right)} \text{ (Pa.s)}$$

Table (1) and figure (2) shows the calculated data using Hirai and Moelwyn-Hughes models. B values are 15667.4 and 33241.6 for Al and Si, respectively.

Table 1: Viscosity according to Moelwyn-Hughes and Hirai models.

x_{Si}	T	A_{Al}	ρ_{Al}	η_{Al}	A_{Si}	ρ_{Si}	η_{Si}	η_{Total}
0	933	2.16E-04	2400	1.6	1.56E-04	2557.8	11.4	1.6
0.05	880	2.11E-04	2415.9	1.8	1.52E-04	2552.3	14.3	2.5
0.12	842	2.07E-04	2427.3	1.9	1.48E-04	2547.7	17.1	4.0
0.2	957	2.18E-04	2392.8	1.6	1.59E-04	2559.9	10.3	3.7
0.3	1084	2.30E-04	2354.7	1.3	1.69E-04	2568.0	6.8	3.3
0.5	1325	2.49E-04	2282.4	1.0	1.87E-04	2568.0	3.8	2.7
0.6	1424	2.56E-04	2252.7	1.0	1.94E-04	2562.1	3.2	2.5
0.65	1479	2.59E-04	2236.2	0.9	1.97E-04	2557.4	2.9	2.4
0.8	1574	2.65E-04	2207.7	0.9	2.03E-04	2546.8	2.6	2.4
0.9	1630	2.69E-04	2190.9	0.9	2.06E-04	2539.0	2.4	2.3
1	1685	2.72E-04	2174.4	0.8	2.09E-04	2530.3	2.2	2.2

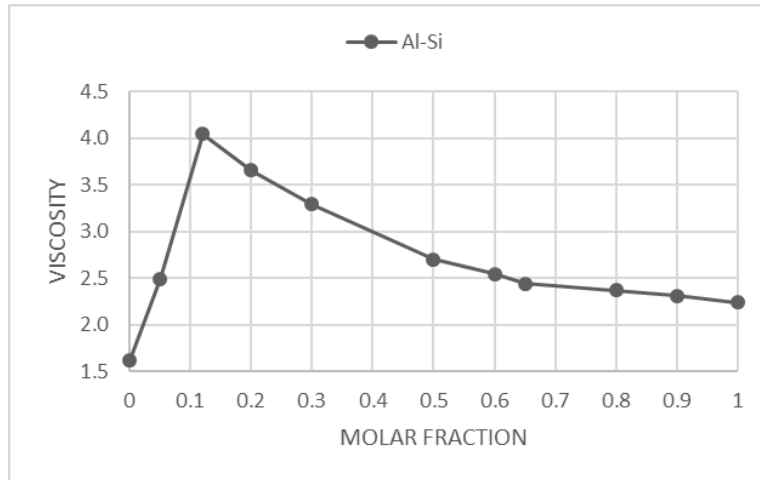


Figure 2: Viscosity of Aluminum-Silicon alloy at different silicon molar fraction.

2.1.3. Surface tension.

According to Kobatake et. al. [24] experimental results, Surface tension of molten Al-Si alloy is illustrated. As shown in figure (3).

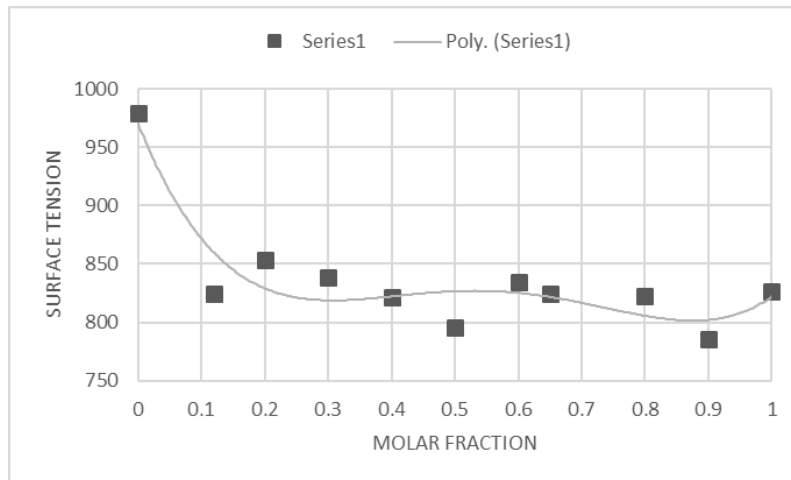


Figure 3: Surface Tension of Al-Si Alloy at different silicon molar fraction.

2.2. Physiochemical properties of water-alcoholic mixtures.

In this section the physiochemical properties of aqueous ethanol and isopropyl mixtures were illustrated. The illustrated data are from literature. Khattab et. al. [20] correlations were used to find properties of water-ethanol mixture. While for

isopropyl density and viscosity, Pang et. al. [21] results were drawn and for surface tension Vazquez et. al. [22] results were used.

2.2.1. Density.

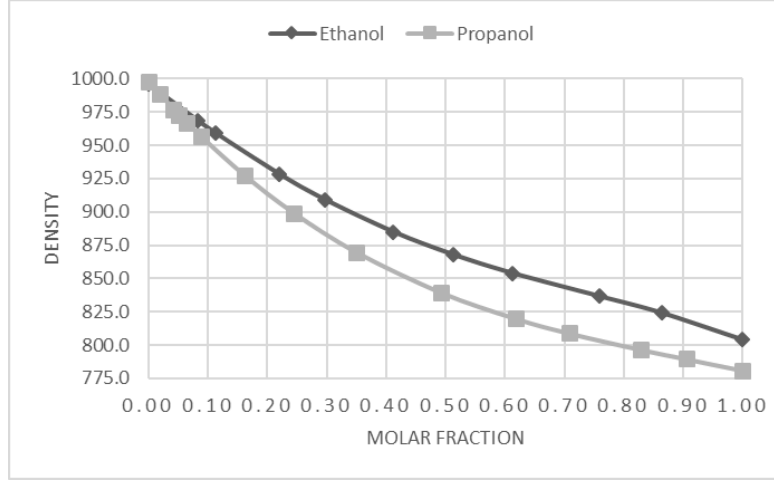


Figure 4: Density (Kg/m³) of water+ethanol and water+2-Propanol mixtures[20], [26].

Figure (4), illustrates the density of water-ethanol and water-isopropyl mixtures. Khattab et. al. [20] correlation which showed in equation (3) was used to find density of water-ethanol mixtures with relative deviation of $0.1 \pm 0.1\%$. where (X_w) , (X_E) , $(\rho_{m,T})$, $(\rho_{E,T})$, $(\rho_{w,T})$ and (T) are water molar fraction, ethanol molar fraction, mixture density, pure ethanol density, pure water density and temperature, respectively. While, for water-isopropyl a regression polynomial equation was constructed according to Pang et. al. [21] experimental results, and has an error of 0.066%. As shown in equation (4). Where (X_p) is 2-propanol molar fraction.

$$\ln(\rho_{m,T}) = X_w \cdot \ln(\rho_{w,T}) + X_E \cdot \ln(\rho_{E,T}) - 30.808 \left[\frac{X_w \cdot X_E}{T} \right] - 18.274 \left[\frac{X_w \cdot X_E \cdot (X_w - X_E)}{T} \right] + 13.89 \left[\frac{X_w \cdot X_E \cdot (X_w - X_E)^2}{T} \right] \quad (3)$$

$$\rho_{m,T} = -0.1616 \cdot X_p^3 + 0.4469 \cdot X_p^2 - 0.5017 \cdot X_p + 0.9975 \quad (4)$$

2.2.2. Viscosity.

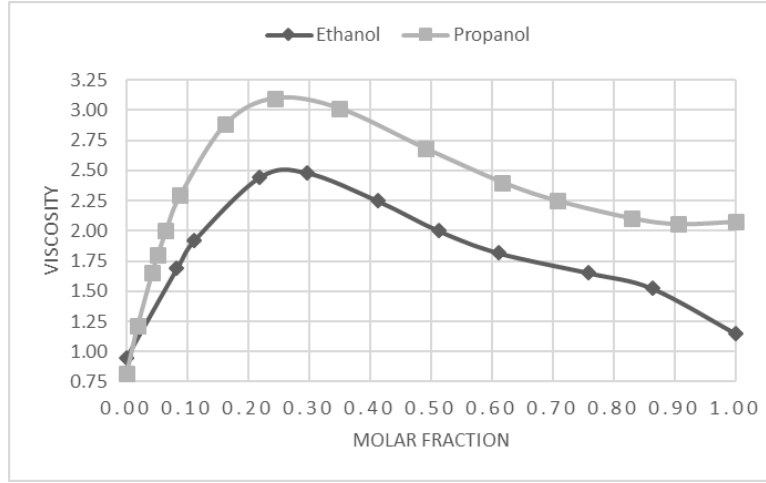


Figure 5: Viscosity of water + ethanol and water + 2-Propanol mixtures [20], [26].

Figure (5), illustrates the viscosity of water-ethanol and water-isopropyl mixtures. Khattab et. al. [20] correlation which showed in equation (5) was used to find Viscosity of water-ethanol mixtures with relative deviation of $10.4 \pm 9.5\%$. Where, $(\eta_{m,T})$, $(\eta_{w,T})$ and $(\eta_{E,T})$ are viscosities of mixture pure water and pure ethanol, respectively. While, for water-isopropyl a regression polynomial equation was constructed according to Pang et. al. [21] experimental results, and has an error of 0.922%. As shown in equation (6).

$$\ln(\eta_{m,T}) = X_w \cdot \ln(\eta_{w,T}) + X_E \cdot \ln(\eta_{E,T}) + 724.652 \left[\frac{X_w - X_E}{T} \right] + 729.357 \left[\frac{X_w \cdot X_E \cdot (X_w - X_E)}{T} \right] + 976.05 \left[\frac{X_w \cdot X_E \cdot (X_w - X_E)^2}{T} \right] \quad (5)$$

$$\eta_m = 26.497 \cdot X_p^5 - 90.964 \cdot X_p^4 + 123.82 \cdot X_p^3 - 81.076 \cdot X_p^2 + 22.978 \cdot X_p + 0.8193 \quad (6)$$

2.2.3. Surface tension.

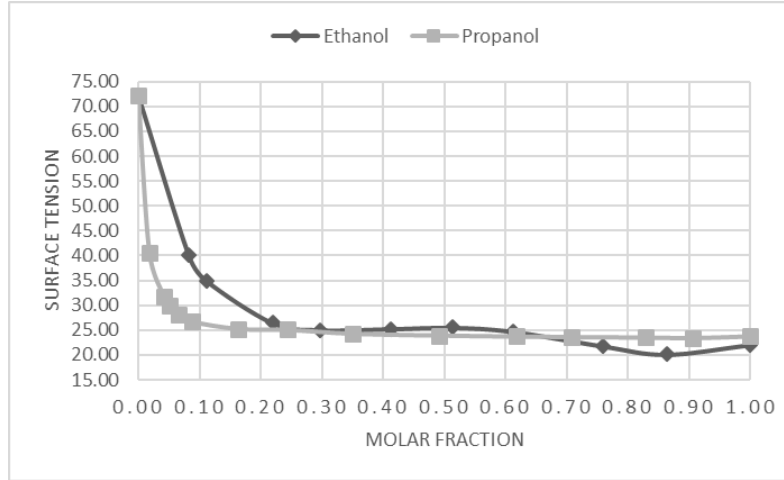


Figure 6: Surface Tension of water + ethanol and water + 2-Propanol mixtures [20],[22].

Figure (6), illustrates the surface tension of water-ethanol and water-isopropyl mixtures. Khattab et. al. [20] correlation which showed in equation (5) can be used to find surface tension of water-ethanol mixtures with relative deviation of $4.2 \pm 3.6\%$. Where (σ) is surface tension. While, for water-isopropyl two regression polynomial equations were constructed according to Vazquez et. al. [22] experimental results. As shown in equations (8) and (9).

$$\ln \sigma_{m,T} = X_w \cdot \ln \sigma_{w,T} + X_E \cdot \ln \sigma_{E,T} - 488.012 \left[\frac{X_w X_E}{T} \right] - 640.785 \left[\frac{X_w X_E (X_w - X_E)}{T} \right] - 1073.31 \left[\frac{X_w X_E (X_w - X_E)^2}{T} \right] \quad (7)$$

$$\sigma_m = -231550 \cdot X_p^5 + 202799 \cdot X_p^4 - 67612 \cdot X_p^3 + 10787 \cdot X_p^2 - 845.21 X_p + 52.709, \text{ for } X_p < 0.3 \quad (8)$$

$$\sigma_m = -4.6785x^3 + 10.697x^2 - 9.1192x + 26.379, \text{ for } X_p > 0.3 \quad (9)$$

2.3. Foaming process in molten metal.

One of the most convenient way to characterize liquid metal foam processing methods is the way described by J.Banhart [27]. In this study the most common methods were illustrated. This study is more interested in direct foaming process which is similar in procedure to the foaming process in alcoholic mixture. Wang et. al. [3] presented a relation for foam stability in molten metal. This relation depends on Surface tension of molten metal, added particles and particles wettability. as shown in equation (10).

$$\sigma_l > \sigma_s \cos \theta \quad (10)$$

Where (σ_l) , (σ_s) and (θ) are liquid phase surface tension, solid phase surface tension and Contact angle between both phases. Also, there are other parameters affect foaming stability which are Size, shape and concentration of added particles. As well as, solid particles must have affinity to gas phase.

2.3.1. Types of foaming processes in molten metal.

- Gas Injection (Direct) (Hydro/Alcan).

Gas injection method is performed by the following steps: firstly, a melt aluminum metal matrix composite is made and calibrated. Then gas is injected and distributed by using a rotating impeller or vibrating nozzle. Finally, the produced foam can be pulled by conveyor. Previous steps were illustrated in Figure (7).

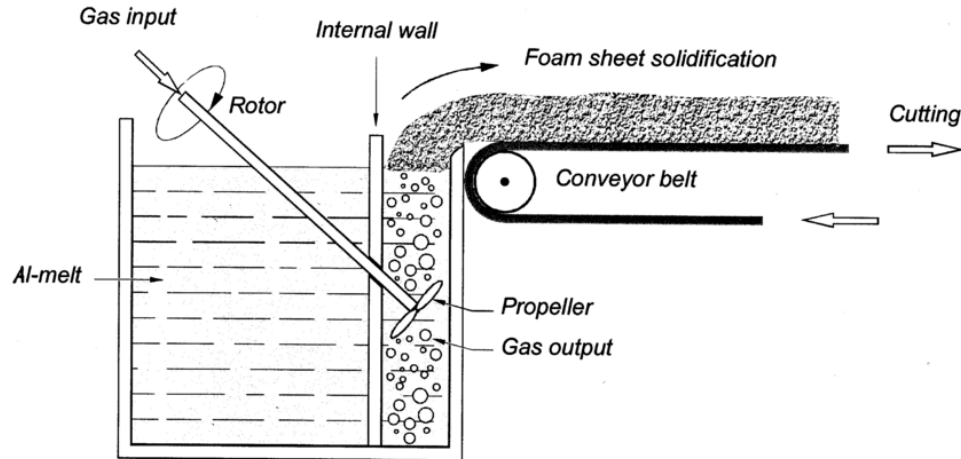


Figure 7: Direct foaming method [27].

- Blowing Agents (Alporas) (melt route) (PM) (Indirect).

Uses blowing agent without gas. By adding additives and stirring the mixture to calibrate the viscosity to a required value. Then adding blowing agent which will react with melt and generate gas which will cause the foaming process.

- Solid-Gas Eutectic Solidification (Gasar).

Depends on eutectic system between hydrogen gas and metal. By using a high-pressure hydrogen atmosphere around the molten metal. Then, gradually cooling the metal causes the mixture of metal-hydrogen reach eutectic state.

- Foaming of Ingots Containing Blowing Agents (Form grip / Foam cast).

It is a combination between Hydro/Alcan and powder metal (another method on powder metal instead of molten one).

2.3.2. Effect of additives and foaming method on metal foam properties.

A summary from the literature for metal foam properties and additives effect are illustrated in tables (2) and (3). At which, Table (3) illustrates the general properties of aluminum foam produced by each method. Whereas, Table (4) presents the effects of additives on the foaming process.

Table 2: Properties of aluminum foam according to production method.

Method	Stabilizer	ρ	Pore size (mm)	Wall thickness	External Gas
(Hydro/Alcan)	Added ceramics	69-540	3-25	0.05- 0.085 (mm)	Air, Nitrogen, Argon
(Alporas)	Oxidation in melt	180 - 240	2-10	-----	No external gas
(Gasar)	Natural viscosity	-----	(0.01-10) dimeter. (0.1-300) length.	-----	Hydrogen
(Formgrip/Foamcast)	Added ceramics	-----	-----	-----	Air, Nitrogen, Argon

Table 3: Different types of additives used in the literature to stabilize aluminum foam.

Ref.	Aluminum Type	Foaming method	Gas type	Used additives and effects		
				Additive	Variable property	Effect
[1] [2]	aluminum alloy A356	Hydro/Alcan	Air	Silicon Carbide SiC	Percentage: 15%	Stability and viscosity
[3]	pure Al	Hydro/Alcan	N2	Silicon Carbide SiC	Percentage: 7-22%	Stability and viscosity
[4]	Aluminum alloy (Al-Si)	Hydro/Alcan	Air	Aluminum oxide Al_2O_3	Particle size and concentration	Cell size
				Silicon Carbide SiC		Cell size and wall thickness.
[5]	Aluminum Powder Al – TiH ₂	Alporas	---	Aluminum oxide Al_2O_3	Foaming Time	Expantivity

2.4. Foaming process in water-alcoholic mixtures.

After the previous explanation regarding physical and chemical properties of water alcoholic mixture, the theory and factors of foaming process had been illustrated in this section. Foam bubbles consists of lamellas and borders, lamellas are bubbles walls while borders are areas confined between bubbles. each bubble is a liquid film which resulted because of balance between several forces. As shown in figure (8).

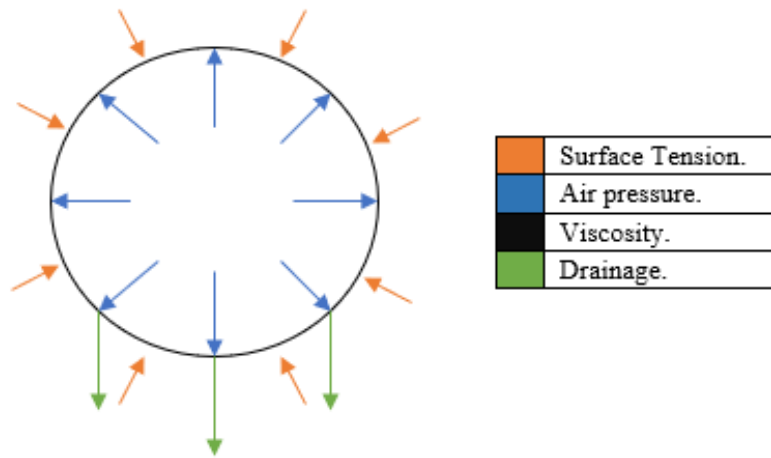


Figure 8: Forces acting on bubble film.

As shown in figure (8), to keep a bubble stable as much as possible, balance is required between surface tension and air pressure. In addition, viscosity provide resistance to the liquid film against drainage caused by gravity; so that higher viscosity leads to slower drainage and longer time for bubble to collapse. H. Kister [28].

Unfortunately, the previously mentioned forces are not enough to explain how do foams last for long time. Which can be hours in some cases. Therefore, an illustration on foaming mechanism in alcoholic mixtures was provided here. According to H. Kister [28] in his book “Distillation operation”, there are two important factors in foaming process: Marangoni effect and Gelatinous layer. Marangoni effect is mass transfer from high surface tension area (liquid) to low

surface tension area (lamellas), this effect is illustrated in following sections. While, the gelatinous layer can be produced manually or due to impurities. Perry stated in his handbook for chemical engineers [29] that any pure liquid shows a foaming tendency, it is due to organic impurities. In this study this effect is negligible because no gel had been used and mixture had been held away from impurities as much as possible.

In addition to previous mentioned factors, there is an interesting rule relate length of used alcohol chains and foam stability which called Traube's rule. This rule states that, surface activity is strongly related to the length of hydrocarbon chains, longer chains lead to higher surface activity and less foam stability.

2.4.1. Viscosity and surface tension effect.

According to Plateau [12] in 1869 best foaming condition should occur at maximum mixture viscosity as higher viscosity leads to lower drainage therefore more stable foam. But further experiments proved this assumption was wrong. And this explained by Marangoni effect that at some point as viscosity goes higher bubbles' lamellas surface tension becomes higher than bulk liquid surface tension which leads to more drainage. Also, Breward et. al. [30] provided relation for Marangoni number which describe Marangoni effect. as shown in table (4).

2.4.2. Magnetic field effect.

To study the magnetic effect on foaming process an ionized mixture must be used. To make an alcoholic mixture ionized salt must be added. Varade et. al. [31] reported the effect of different salts and oil on foaming process and they found that, surface tension and foam stability were decreased significantly. In their study, they used an aqueous solution of zwitterionic surfactant which is considered a strong foaming agent. In this study, when salt is added to the mixture no foaming process occurred even at best foaming condition. That is because alcoholic aqueous solution

is considered relatively weak foaming mixtures. For investigation of magnetic field on foaming process a more stable foaming mixtures are recommended.

2.4.3. Collapse time.

As mentioned before in introduction, F. Schutz [15] performed an experiment on collapse time which defined as foam disappearance of middle of experimental tube. His experiment produced foam by shaking of a closed tube containing foaming mixture, then time is calculated for foam to disappear.

His results showed that isopropyl mixture only foamed at a two volume fractions: The first one is at 0.005 volume fraction with good collapse time of 18 seconds. the second fraction is at 0.3 volume fraction with a very unstable foam which have collapse time of 3.6 seconds. Also, he provided a correlation which relate with good accuracy collapse time with number of carbon atoms valid only for a primary alcohol.

2.4.4. Drainage rate.

Drainage is a result of gravitational forces and Marangoni effect. According to Bikerman [32], equation (11) and its derivation (12) illustrate a relation for drainage rate for several systems. Where, Q_0 is initial foam volume and Q is drained volume after time (t). Constant (k) can be found by equation (13) experimentally. To use these relations drained volume and foam initial volume should be measured experimentally.

$$\frac{Q}{Q_0} = \frac{t}{\frac{t}{Q_0} + k} \quad (11)$$

$$\frac{\partial V}{\partial t} = \frac{k Q_0^2}{t + k Q_0^2} = \frac{k Q^2}{t} \quad (12)$$

$$2kt = \frac{1}{(Q_0 - Q)^2} - \frac{1}{Q^2} \quad (13)$$

According to Breward et. al. [30] several dimensionless numbers can be calculated depending on drainage velocity which are Reynolds, capillary and Marangoni Numbers. These numbers with their definition are illustrated in table (4). Where (L) is bubble lamella length for lamella dominated foam or plateau border length for border dominated foam, (U) drainage velocity through lamella, ν is kinematic viscosity and $\Delta\sigma$ is surface tension difference between bulk fluid and lamella's surface tension.

Table 4: Dimensionless parameters which describe a bubble on liquid surface.

Reynolds	$\frac{\rho L U}{\eta}$	$\frac{\text{inertial forces}}{\text{viscous forces}}$
Marangoni	$\frac{\Delta\sigma}{\eta U}$	$\frac{\text{advective rate (surface tension difference)}}{\text{diffusive rate (viscosity)}}$
Capillary	$\frac{\eta U}{\sigma}$	$\frac{\text{Viscous forces}}{\text{surface tension forces}}$

In this study the relations provided by P.Stevenson [33] and Neethling et. al. [34], were used to calculate the drainage velocity. Borders Area (A_{bo}) according to P.Stevenson [33] are considered area confined between three circles and its relation is shown in equation (14).

$$A_{bo} = 0.162 r_c^2 \quad (14)$$

Where (r_c) is radius of curvature which has a relation to bubble radius (r_b) and liquid volume fraction of the foam $\left(\frac{Q_l}{Q_T}\right)$, where (l) and (T) represents liquid and total foam volume. as shown in equation (15).

$$r_c = 1.28 r_b \left(\frac{Q_l}{Q_T}\right)^{0.46} \quad (15)$$

Neethling et. al. [34] had proposed a relation to calculate lamellas length (L) as shown in equation (16).

$$L = 0.718 \frac{r_b}{\left(1 - \frac{Q_L}{Q_T}\right)^{\frac{1}{3}}} \quad (16)$$

Using previous equations (14) to (16) with experimentally calculated drainage rate using equations (11) to (13), the dimensionless numbers in table (4) can be calculated. This calculation with a proposed relation for drainage velocity is illustrated in this study results.

2.4.5. Defoaming agents.

According to H. Kister [28] in his book, most commonly used defoaming agents are silicones which are solid and prevent surface flow of the bulk mixture to the bubbles (cease Marangoni effect) and mixes within foam thin layers causing it to collapse. Also, there are some studies on synthetic organic compounds which prevent foaming. Asbeck et. al. [35] got a patent on such a compound which is a long series ketone or secondary alcohol (more than 22 carbon atoms), according to Trabue's rule a compound of such a carbon chain length should have a dramatic reduction on foam stability.

3. Experimental setup.

The equipment and tools for experimental setup are shown in figure (9). The used storage is translucent painted with unreflective black paint except for a small area at which led light is mounted. Storage translucency helped to diffuse the lid light so that it would reflect within all storage.

Polarization filters were used to eliminate specular reflections. Three filters were used for camera, led light source and for camera's flashlight. Filters were attached in opposed directions to assure the cross-polarization effect, this effect is illustrated in figure (10).

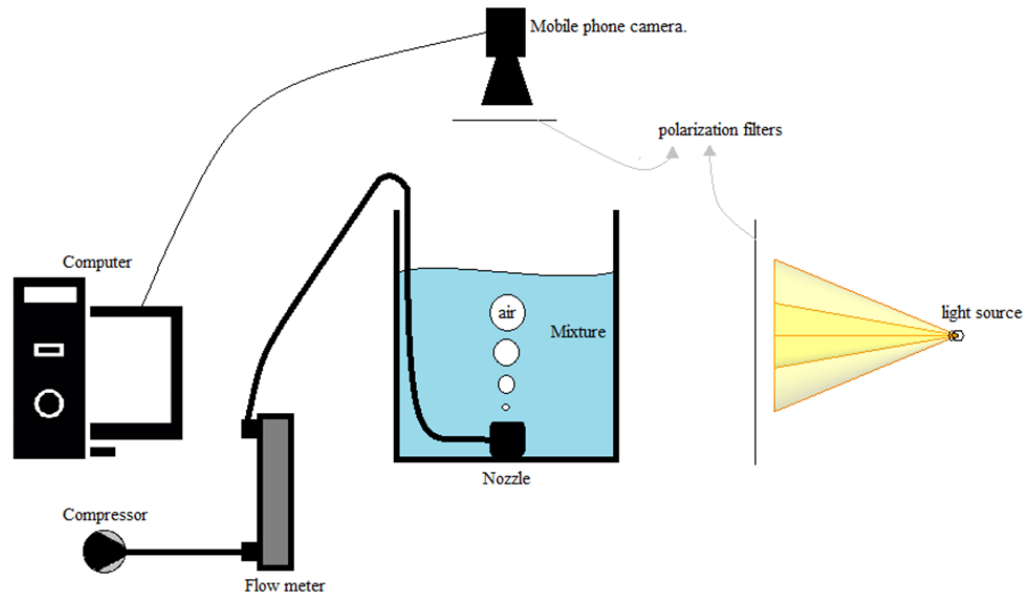


Figure 9: Experimental setup.

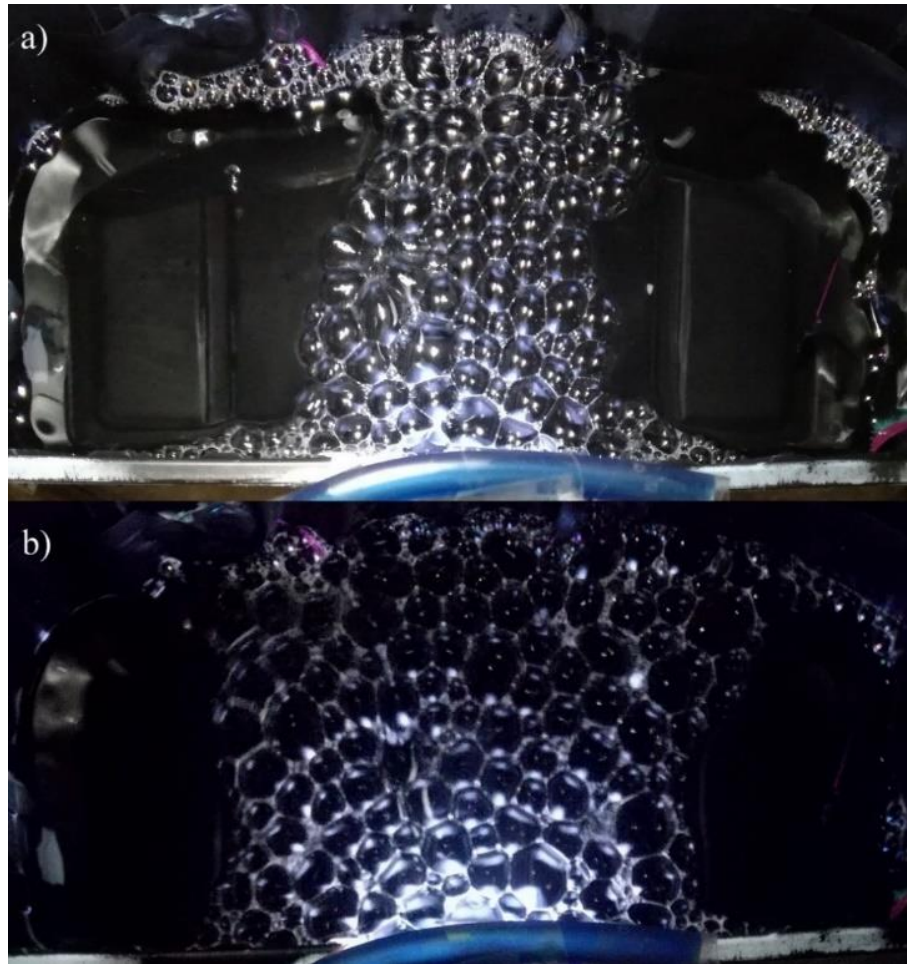

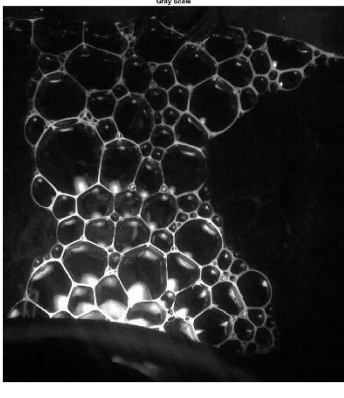
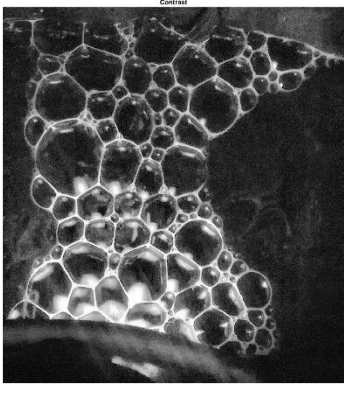
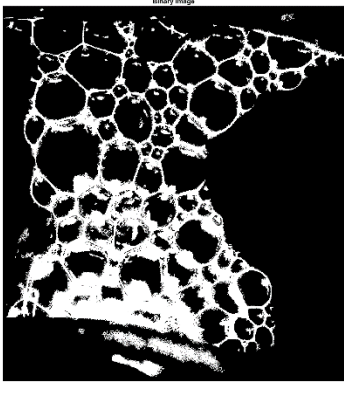


Figure 10: Cross polarization effect. Images where taken by Huawei P9 lite camera and flashlight of Samsung S5 was used. a) unpolarized image, b) Polarized image.

For measured properties, Viscosity where measured by A&D company limited viscometer SV-10 series. Density where measured using DMA 35 density meter. For image processing, Matlab Image processing Toolkit was used. The used Code provide a tabulated results of bubbles diameter and numbers with histograms. Table (5) illustrates image preprocessing steps and the used code is shown in annex (1). The experiment was performed in three parts as shown below.

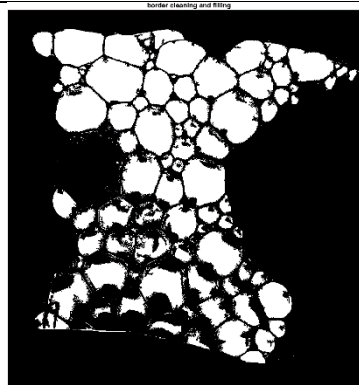
Table 5: Image preprocessing steps.

Original image.	
Gray scale.	
Contrast.	
Switch to Binary image.	

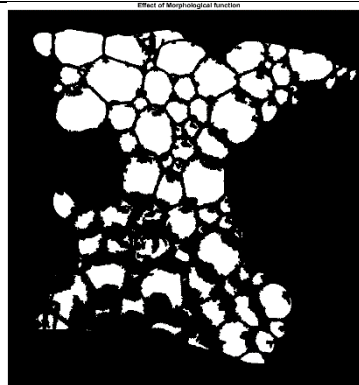
Switch between black and white.



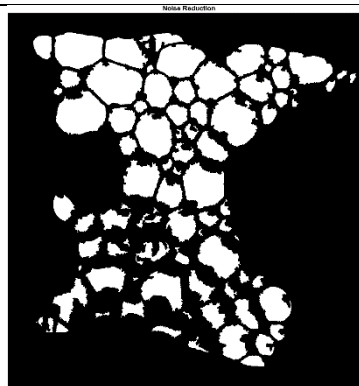
Border cleaning and filling.

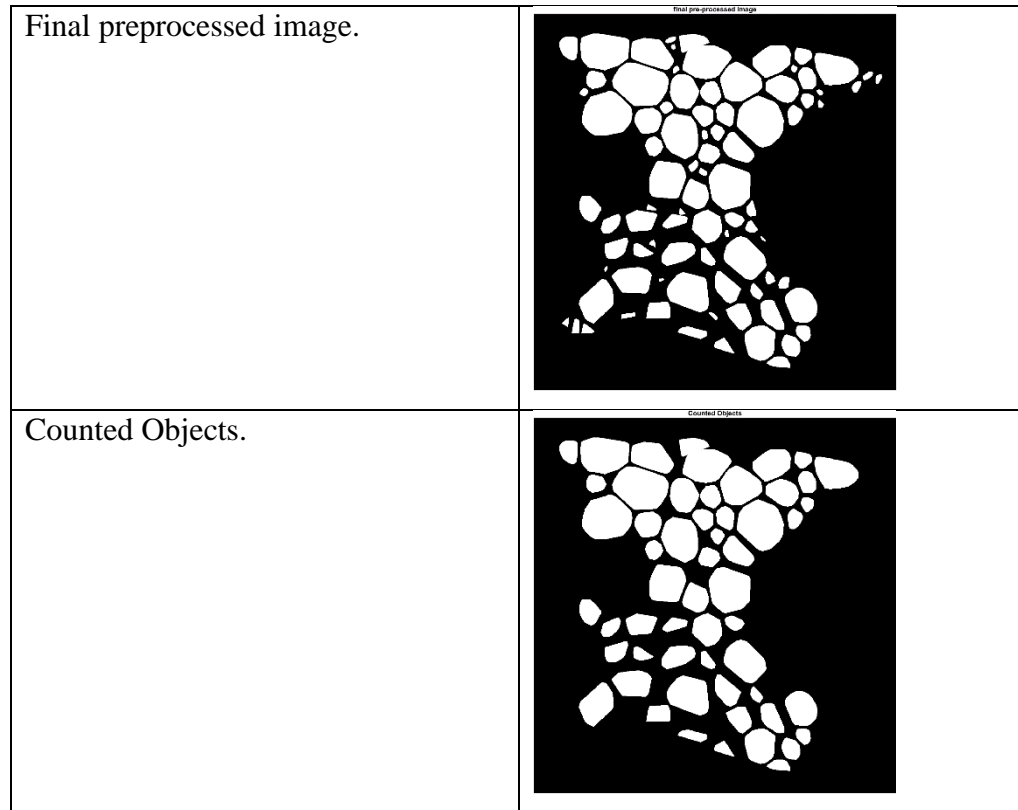


Effect of morphological function.



Noise reduction.





3.1. Part one: Best foaming condition.

In this part air is injected into the mixture for 20 seconds and flow rate of 50 L/h from a 4mm nozzle at different ethanol volume fractions then images were taken at each fraction, as well as density and viscosity were measured. After that, the developed code was used for Image processing to find diameters and numbers of created bubbles; to decide which is the best volume fraction for foaming process.

3.2. Part two: flow rate and foaming time effect.

In this part bubbles' diameters and numbers were measured at different flow rate (15, 25, 50 and 75 L/h) and foaming time (20, 35 and 55 seconds); to investigate foaming time and flow rate effect on diameter and number of bubbles.

3.3. Part three: calculation of drainage velocity.

In this part the same nozzle is added to 250ml measuring tube and filled with 150ml of best foaming mixture. After 30 seconds foaming time at different flow rate (15, 25, 50 and 75 L/h), collapse time was recorded starting by turning off the compressor and ended when first bubble on liquid surface rupture.

Then drainage velocities were calculated by using the following proposed method. The drainage flow rate is considered constant due to short collapse time and low foam liquid volume (dry foam). So, drainage velocity can be written in the following form:

$$U = \frac{Q_L}{t A_{eff}} \quad (17)$$

Where (Q_L) is liquid volume of the foam, (t) collapse time and (A_{eff}) is cross sectional area at which liquid flows. This area is a summation of lamella's and borders cross sectional areas.

At each cross section through the foam there are units of lamellas and borders coexist together which form bubbles. Giving these bubbles (N_u) number and considering each of them have constant cross-sectional Area (A_u). Therefore, the effective area (A_{eff}) can be written as shown in equation (18). Also, (N_u) can be expressed by dividing liquid content in these bubbles ($Q_{L,u}$) over liquid content of one bubble (Q_u) as shown in equation (19). And (Q_u) can be written as shown in equation (20). Where L is lamella length as described by Neethling et. al. [34].

$$A_{eff} = A_u N_u \quad (18)$$

$$N_u = \frac{Q_{L,u}}{Q_u} \quad (19)$$

$$Q_u = A_u L \quad (20)$$

And as an approximation the liquid content in these bubbles can be written as a ratio between bubbles mean diameter and foam thickness. As shown in equation (21). Where ($Q_{l,u}$) is water content in bubbles at the required cross section, (D_b) is bubble diameter and (H) is foam thickness. Combining previous equations with Neethling relation for lamella's length result into equation (22) for drainage velocity.

$$\frac{Q_{l,u}}{Q_l} = \frac{D_b}{H} \quad (21)$$

$$U = \frac{0.36 H}{t \left(1 - \frac{Q_l}{Q_T}\right)^{\frac{1}{3}}} \quad (22)$$

Equation (22) were used for this study to find drainage velocity and dimensionless parameters shown in table (4).

3.4. Part four: similarities between foaming process in water-ethanol mixture and Al-Si alloy.

In this section a comparison of physiochemical properties between best foaming condition of alcoholic mixture and foaming process in Al-Si alloy was presented. Properties were nondimensionalized with respect to pure water and molten aluminum properties. The used data for foaming in molten Al-Si alloy are from Fangming et. al. [36] experimental data for direct foaming process. They used A356 Al-Si alloy at temperature of (1053 K) and SiC volume fraction between 5% and 20%.

4. Results.

4.1. Part one: Best foaming condition.

Table (6) and (7) illustrates the measured results and table (8) indicates the processed images which mentioned in table (6).

Table 6: Measured properties for water ethanol mixture.

Water-Ethanol												
Q		V		X		T	ρ	η	σ	Image No	N	D_b
Q_w	Q_E	V_w	V_e	X_w	X_e							
1000	0	1.00	0.00	1.00	0.00	298	995.8	0.95	72.15	-	-	-
1000	50	0.95	0.05	0.98	0.02	296	990.8	1.07	63.49	1	90	4.8
1000	100	0.91	0.09	0.97	0.03	297	985.6	1.20	56.77	2	143	4.3
1000	175	0.85	0.15	0.95	0.05	297	978.6	1.37	49.17	3	155	5.3
1000	250	0.80	0.20	0.93	0.07	297	973.6	1.53	43.70	4	148	3.8
1000	450	0.69	0.31	0.88	0.12	298	967.1	1.99	33.24	-	-	-
0	1	0.00	1.00	0.00	1.00	298	804	1.05	22.07	-	-	-
a) Surface tension values are from literature. b) Foam appeared only between 0.05 to 0.3 of ethanol volume fraction. c) Bubbles were only stable at 0.15 ethanol volume fraction. While at other fractions bubbles disappeared quickly. d) Images were taken at top view.												

Table 7: Measured properties for water isopropyl mixture.

Water-Isopropyl									
Q		V		X		T	ρ	η	σ
H ₂ O	C ₃ H ₈ O	V _w	V _p	X _w	X _p				
1000	0	1.000	0.000	1	0	298	995.8	0.95	72.15
1400	100	0.933	0.067	1.4	0.1	297	989.10	1.19	41.15
1400	0150	0.903	0.097	1.4	0.15	297	985.10	1.35	37.23
1400	250	0.848	0.152	1.4	0.25	298	977.47	1.64	31.97
1400	350	0.800	0.200	1.4	0.35	298	970.30	1.89	25.89
1400	500	0.737	0.263	1.4	0.5	299	960.33	2.19	25.72
700	300	0.700	0.300	0.7	0.3	298	954.17	2.36	25.61
0	1000	0.000	1.000	0	2	295	781.10	2.07	23.75
a) Surface tension values are from literature. b) Foam did not appear for water iso-propyl mixture.									

In figure (11), the measured densities and viscosities are plotted with ethanol isopropyl volume fractions. The measurement had been started with 1 L of water then ethanol was added gradually by amounts shown in table (5) and foaming process at each point was repeated for 3 or 4 times to assure the results. Densities and viscosities were measured after 5 minutes of mixing. There is approximately 3 seconds between turning of the compressor and taking the image at each point.

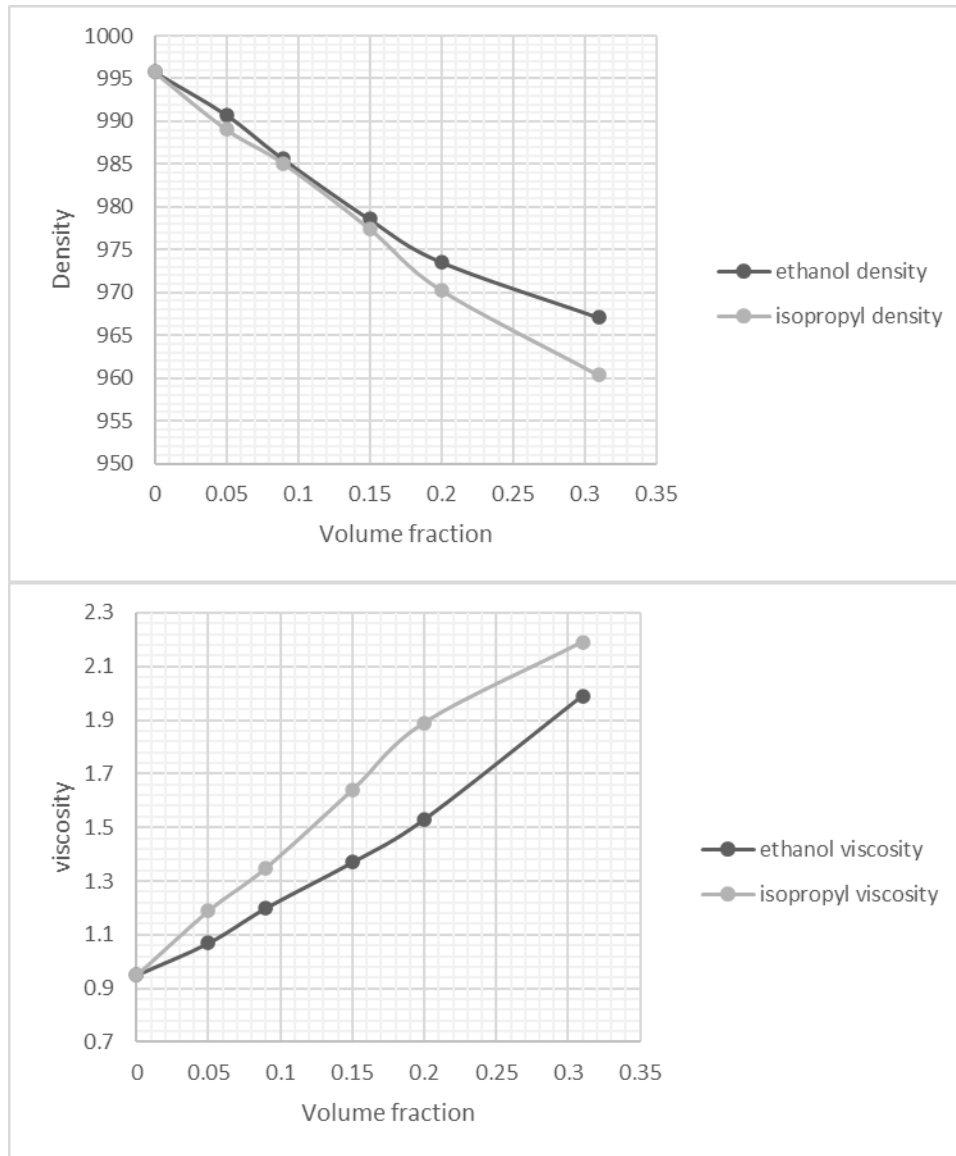
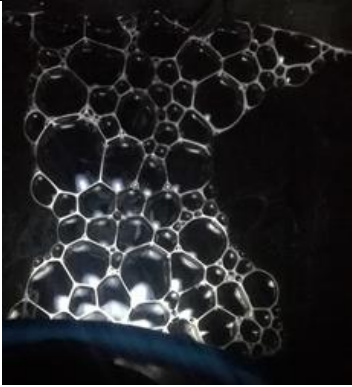

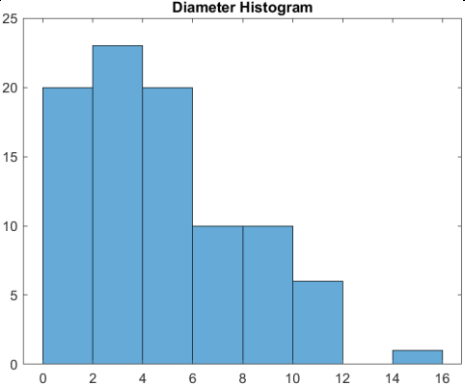
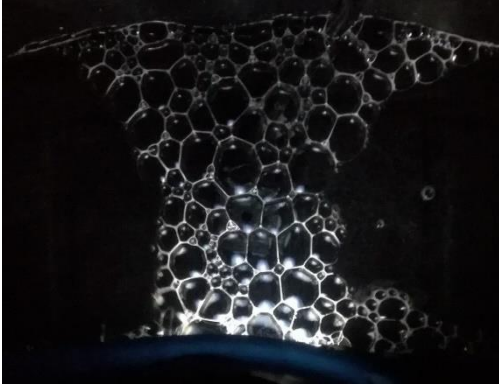
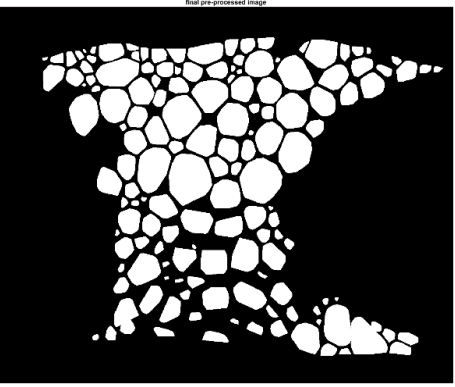
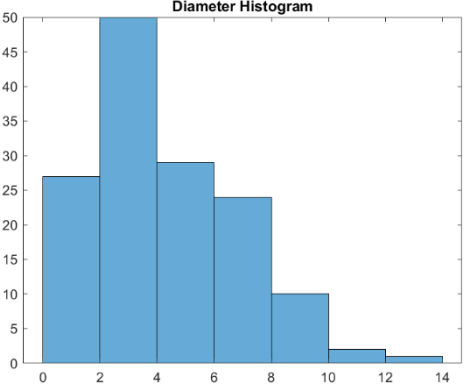
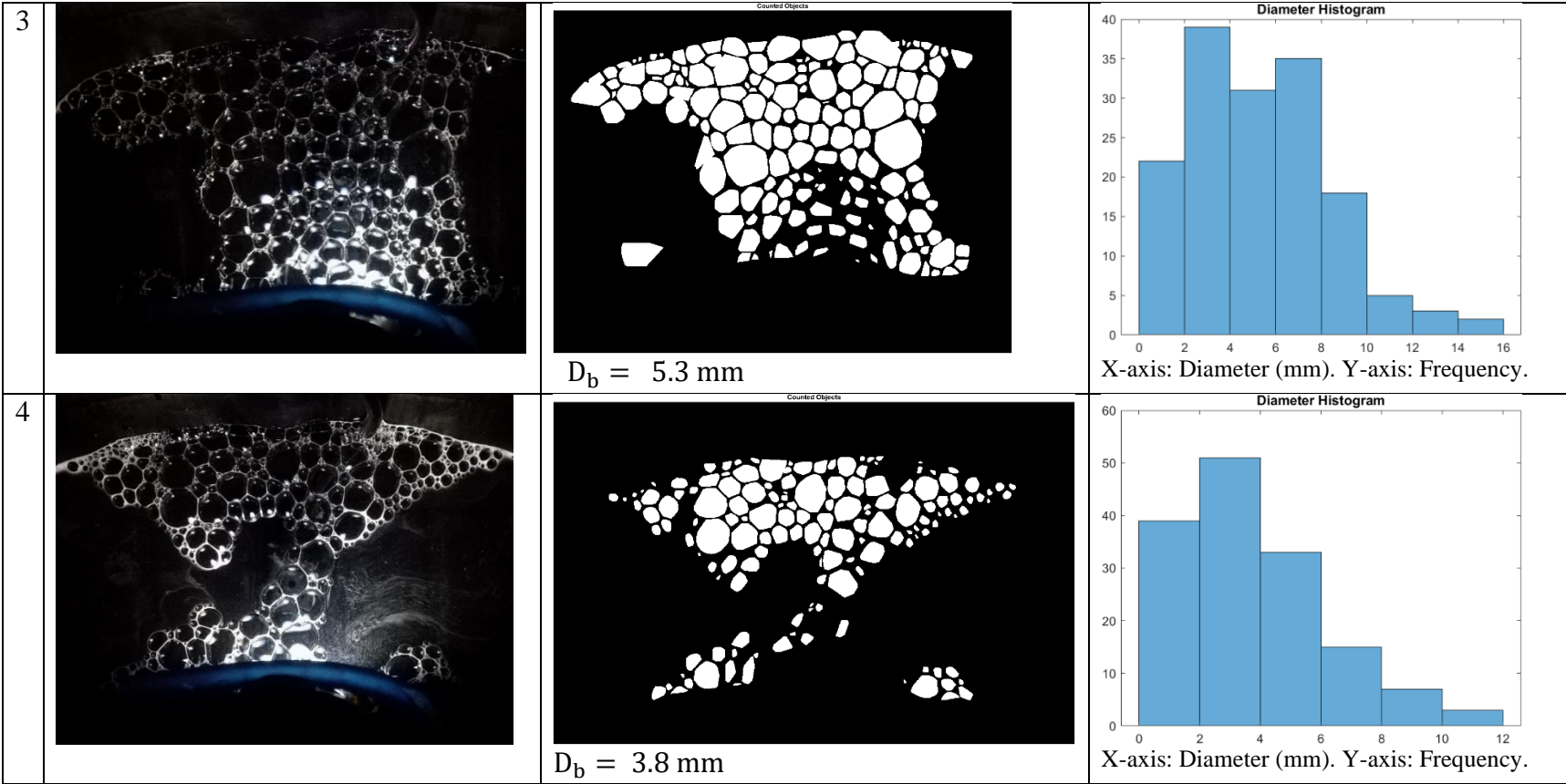


Figure 11: Comparison between measured data for isopropyl and ethanol mixtures.

Table 8: Part one results.

	Original image	Processed image	Diameter histogram.																		
1		 $D_b = 4.8 \text{ mm}$	 <p>Diameter Histogram</p> <p>X-axis: Diameter (mm). Y-axis: Frequency.</p> <table border="1"> <caption>Data for Diameter Histogram 1</caption> <thead> <tr> <th>Diameter (mm)</th> <th>Frequency</th> </tr> </thead> <tbody> <tr><td>0-2</td><td>20</td></tr> <tr><td>2-4</td><td>23</td></tr> <tr><td>4-6</td><td>20</td></tr> <tr><td>6-8</td><td>10</td></tr> <tr><td>8-10</td><td>10</td></tr> <tr><td>10-12</td><td>6</td></tr> <tr><td>12-14</td><td>0</td></tr> <tr><td>14-16</td><td>1</td></tr> </tbody> </table>	Diameter (mm)	Frequency	0-2	20	2-4	23	4-6	20	6-8	10	8-10	10	10-12	6	12-14	0	14-16	1
Diameter (mm)	Frequency																				
0-2	20																				
2-4	23																				
4-6	20																				
6-8	10																				
8-10	10																				
10-12	6																				
12-14	0																				
14-16	1																				
2		 $D_b = 4.3 \text{ mm}$	 <p>Diameter Histogram</p> <p>X-axis: Diameter (mm). Y-axis: Frequency.</p> <table border="1"> <caption>Data for Diameter Histogram 2</caption> <thead> <tr> <th>Diameter (mm)</th> <th>Frequency</th> </tr> </thead> <tbody> <tr><td>0-2</td><td>27</td></tr> <tr><td>2-4</td><td>50</td></tr> <tr><td>4-6</td><td>29</td></tr> <tr><td>6-8</td><td>24</td></tr> <tr><td>8-10</td><td>10</td></tr> <tr><td>10-12</td><td>2</td></tr> <tr><td>12-14</td><td>1</td></tr> </tbody> </table>	Diameter (mm)	Frequency	0-2	27	2-4	50	4-6	29	6-8	24	8-10	10	10-12	2	12-14	1		
Diameter (mm)	Frequency																				
0-2	27																				
2-4	50																				
4-6	29																				
6-8	24																				
8-10	10																				
10-12	2																				
12-14	1																				



4.2. Part two: flow rate and foaming time effect.

Best foaming mixture at different flow rate and foaming time was summarized in table (9). Effect of foaming time and flow rate on bubbles number and diameter were plotted in figure (12) and (13), respectively. Processed images of part two were illustrated in table (10).

Table 9: Results of processed images for part 2.

Flow rate (L/h)	foaming time (s)	Number of bubbles	D_b
15	20	162	3.9
	35	190	4
	55	245	4
25	20	120	4.46
	35	187	4.6
	55	223	4.46
50	20	151	5.24
	35	216	5
	55	305	4.8
75	20	238	3.9
	35	246	4.46
	55	259	4.1

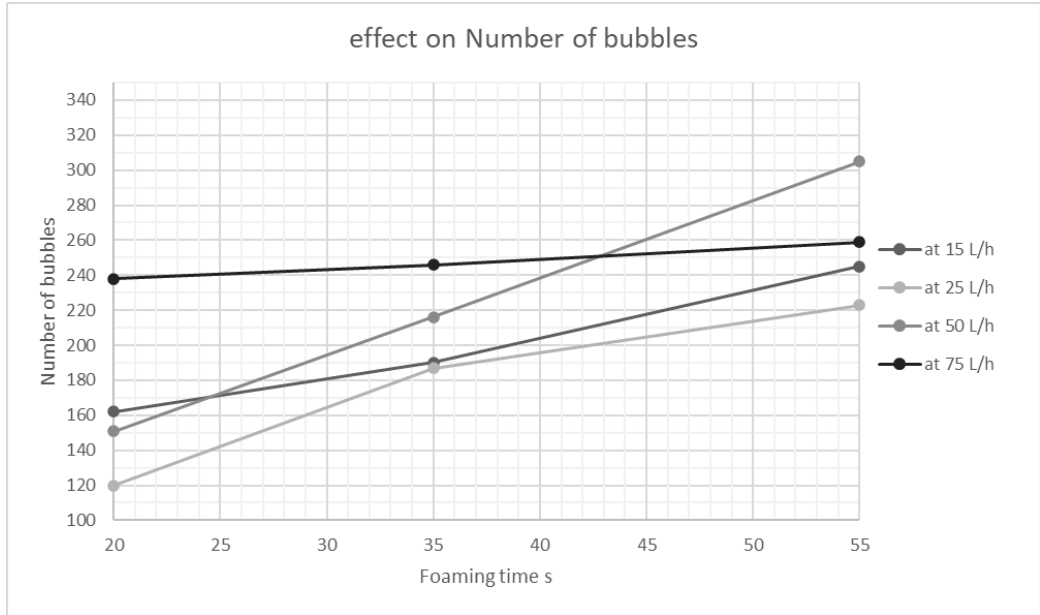


Figure 12: Foaming time and flow rate effect on number of bubbles.

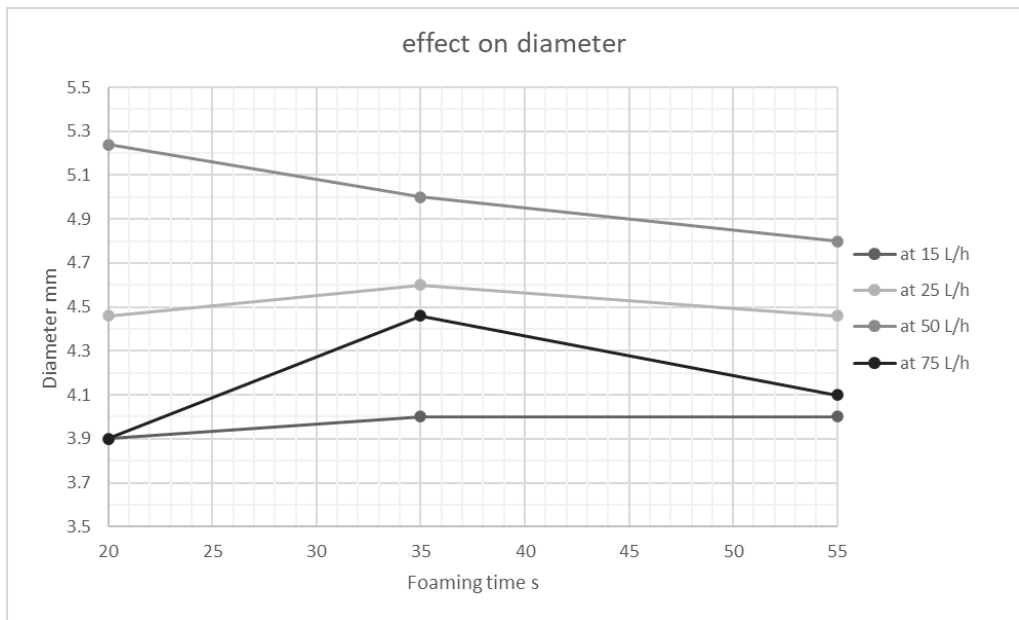
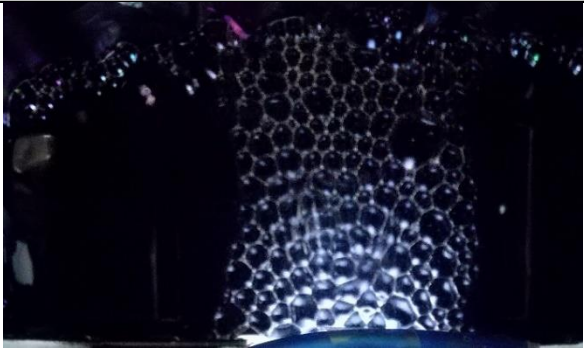
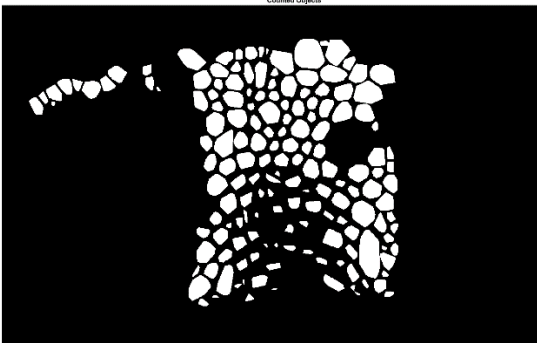
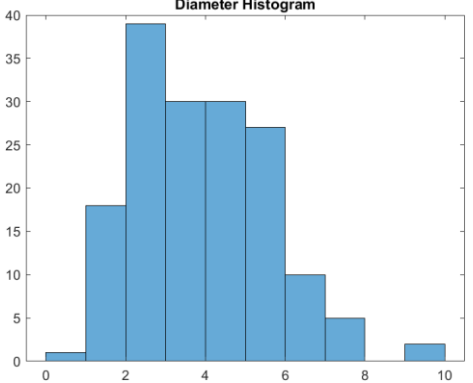
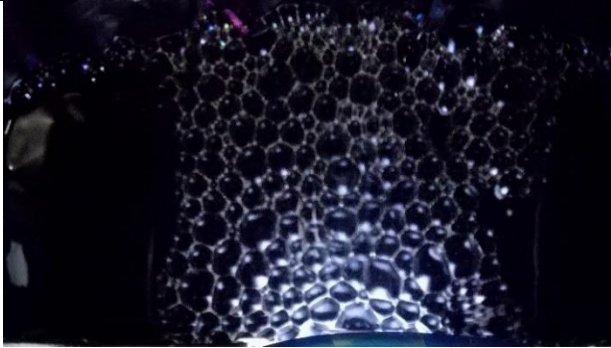
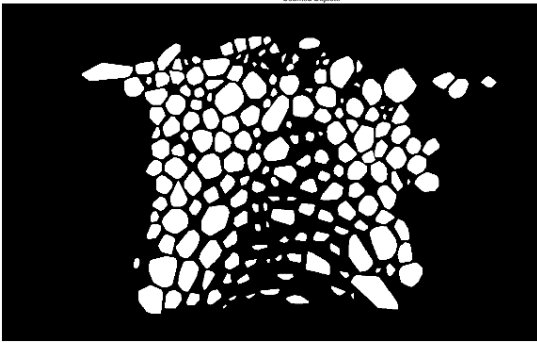
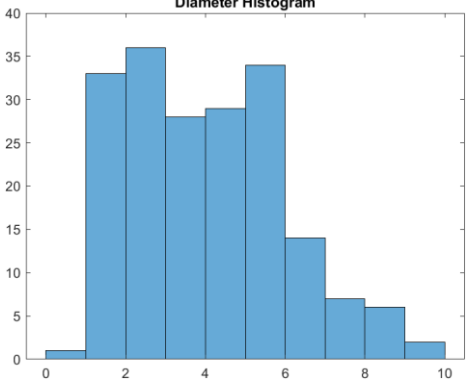
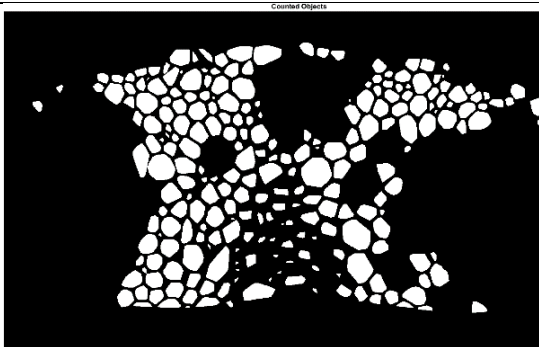
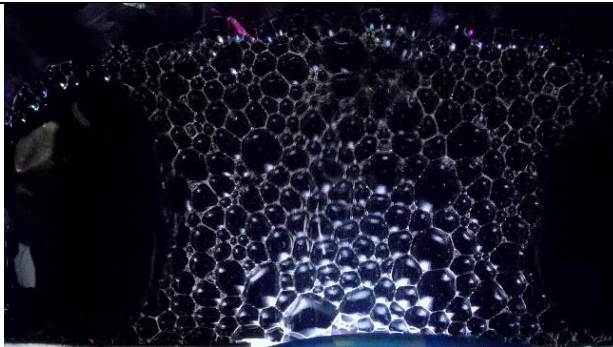


Figure 13: Foaming time and flow rate effect on diameter.

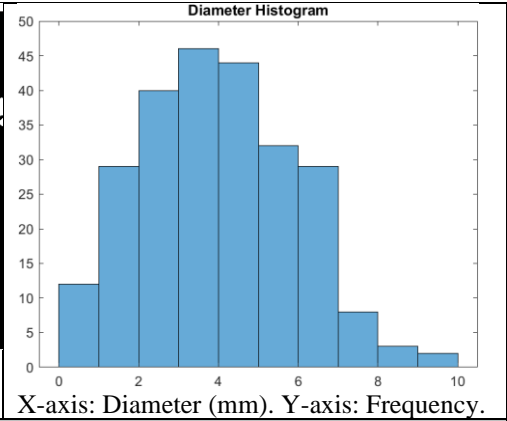
Table 10: Part two results.

	Original image	Processed image	Histogram
15 L/h			
20 s		 <p>$D_b = 3.9$ mm, Number of bubbles = 162</p>	 <p>X-axis: Diameter (mm). Y-axis: Frequency.</p>
35 s		 <p>$D_{m.exp} = 4$ mm, Number of bubbles = 190</p>	 <p>X-axis: Diameter (mm). Y-axis: Frequency.</p>

55
s

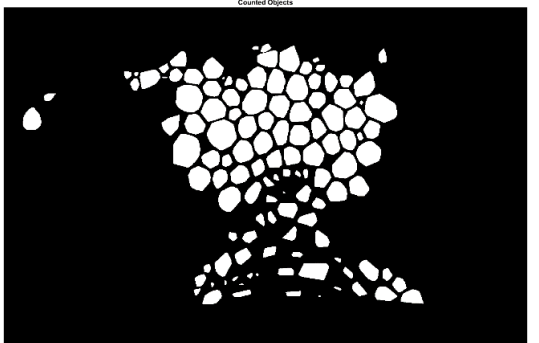
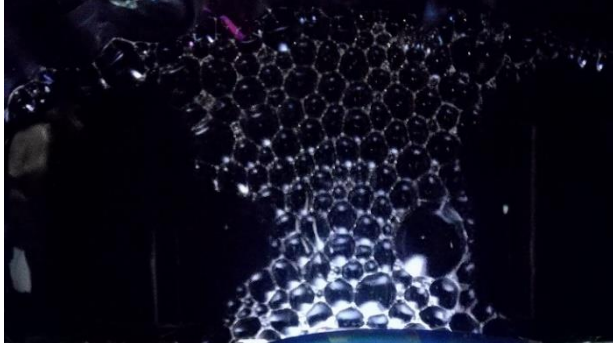


$D_b = 4$ mm, Number of bubbles = 245

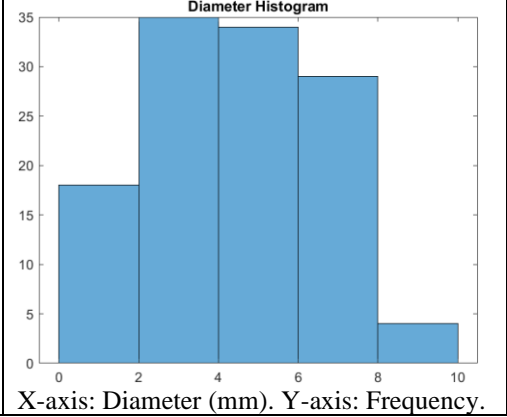


25 L/h

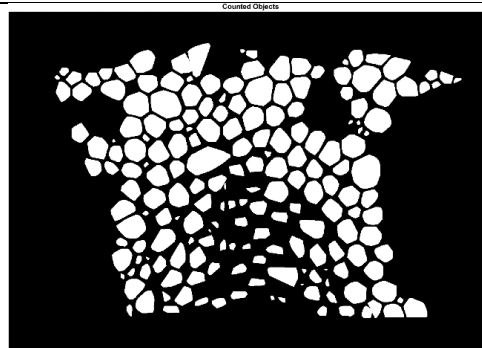
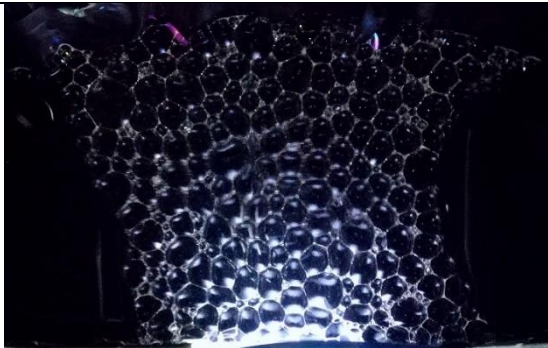
20
s



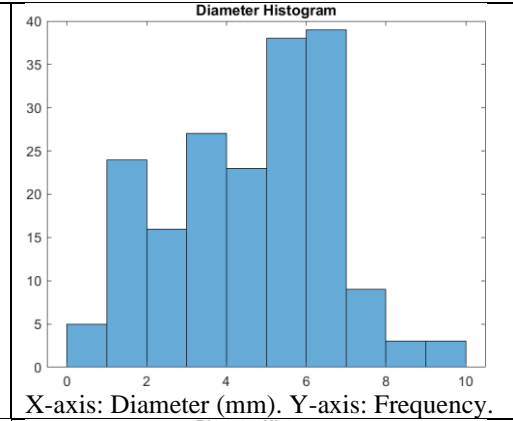
$D_b = 4.46$ mm, Number of bubbles = 120



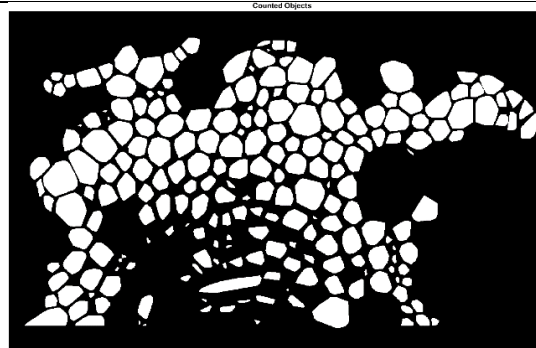
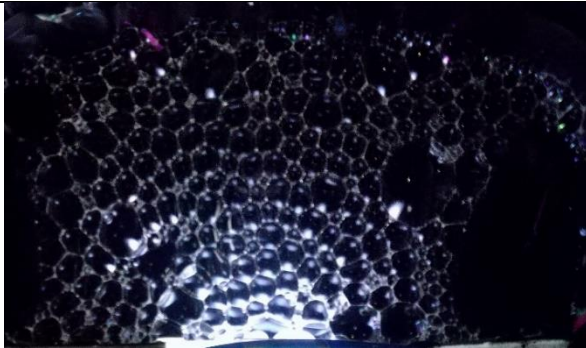
35
s



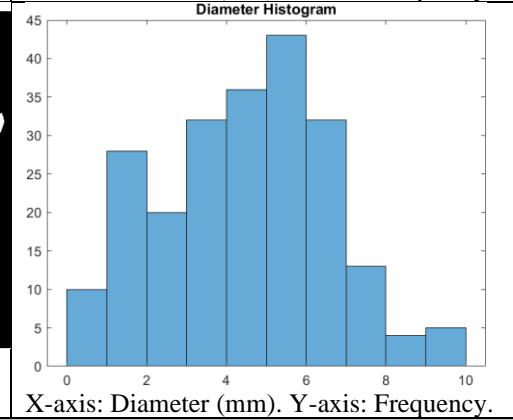
$D_b = 4.6$ mm, Number of bubbles = 187



55
s

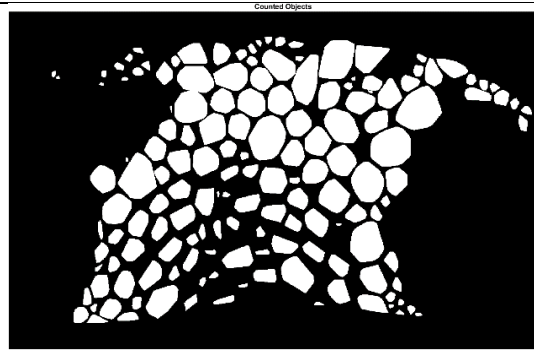
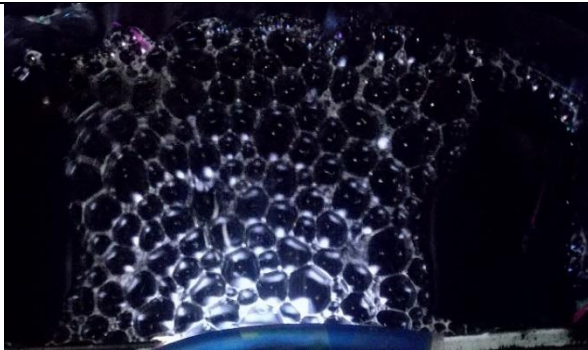


$D_b = 4.46$ mm, Number of bubbles = 223

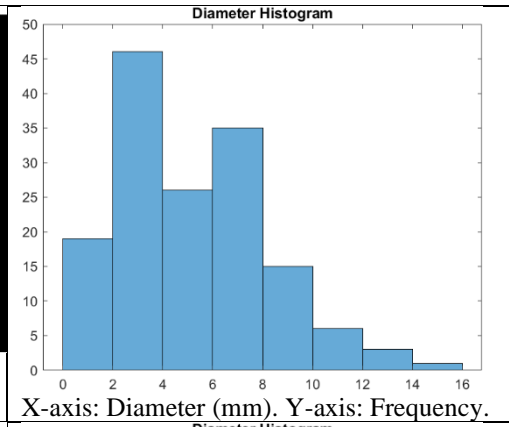


50 L/h

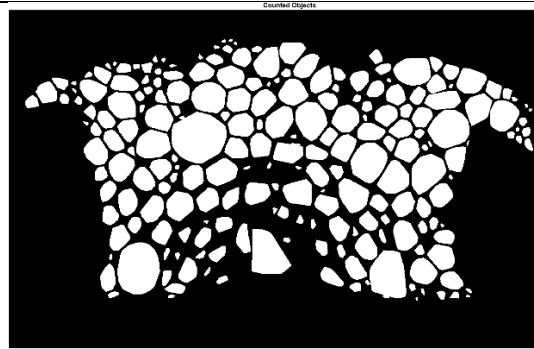
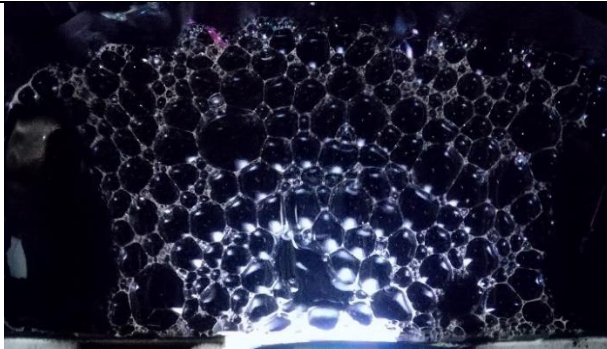
20
s



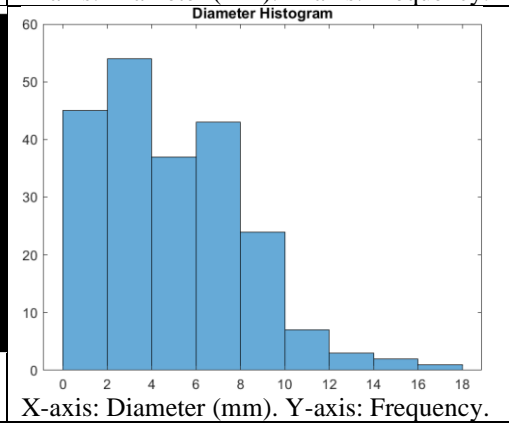
$D_b = 5.24$ mm, Number of bubbles = 151



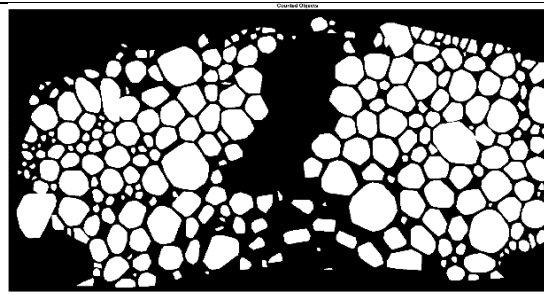
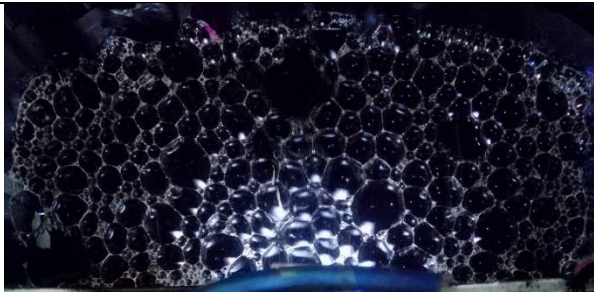
35
s



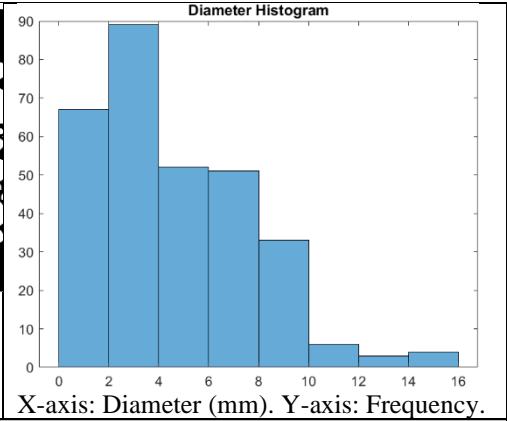
$D_b = 5$ mm, Number of bubbles = 216



55
s

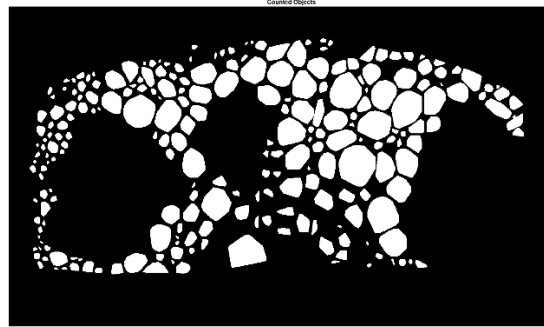
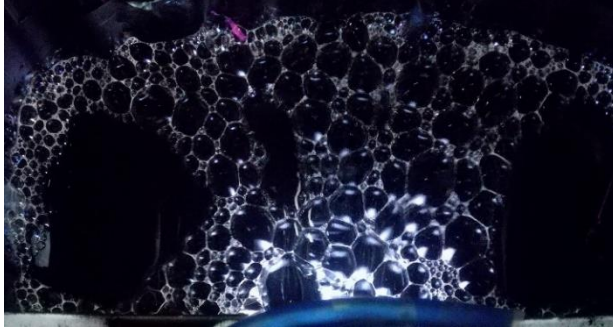


$D_b = 4.8$ mm, Number of bubbles = 305

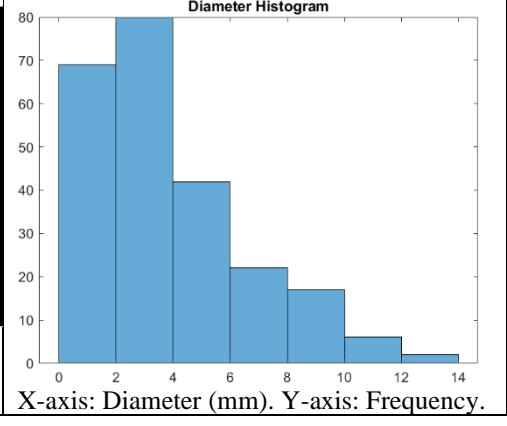


75 L/h

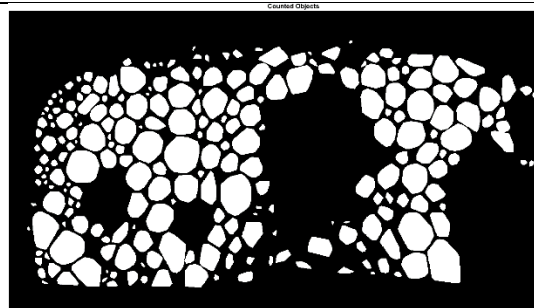
20
s



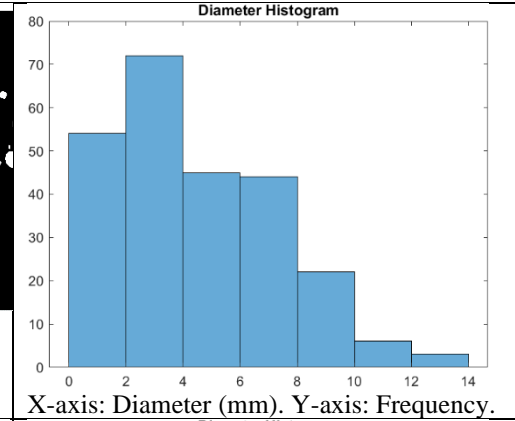
$D_b = 3.9$ mm, Number of bubbles = 238



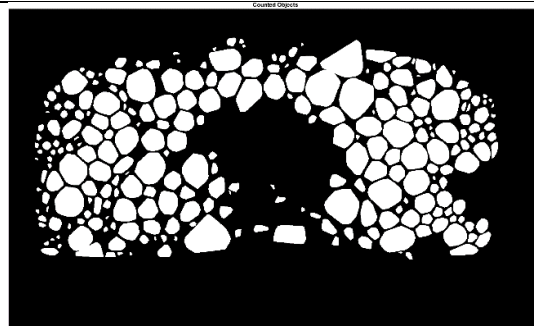
35
s



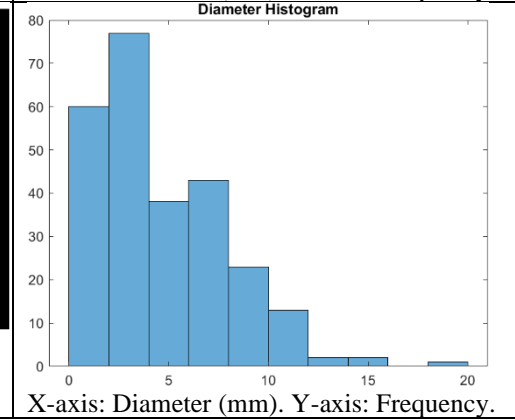
$D_b = 4.46$ mm, Number of bubbles = 246



55
s



$D_b = 4.75$ mm, Number of bubbles = 259



4.3. Part three: calculation of drainage velocity.

The proposed relation for drainage velocity was used with measured data to find Capillary (C_a), Marangoni (M_r) and Reynold's (R_e) Numbers. The results are illustrated in table (11).

Table 11: Part three results: drainage rate and dimensionless parameters.

Flow rate (L/h)	r_b (mm)	Q_t (ml)	Q_L (ml)	H (mm)	t (s)	U (mm/s)	Ca	Mr	Re
15	2	35	1.00	21	18	2.12	1.17E-04	4709.7	6.0
25	2.25	50	1.50	30	25	2.18	1.20E-04	4578.9	6.9
50	2.5	70	2.00	42	32	2.39	1.32E-04	4186.4	8.4
75	2.35	90	2.50	54	56	1.75	9.67E-05	5698.2	5.8
<ul style="list-style-type: none"> • Foaming time is 30 seconds for each flow rate. • Measured values are t which is the collapse time measured when the compressor is turned off until the rupture of first bubble on liquid surface occurred, H is foam thickness, Q_t foam total volume and Q_L is liquid content in the foam (this value could not be measured because it is very low for dry foam so these are arbitrary values). • r_b is bubble mean diameter as measured in section 4.2. 									

4.4. Part four: similarities between foaming process in alcoholic mixture and Al-Si alloy.

The shown properties in table (12) are dimensionless by dividing them on their values for pure water or aluminum. Properties for water-ethanol mixture were measured experimentally at best foaming condition except for surface tension it was taken from Vazquez et. al. [22] study. While for molten Al-Si alloy, Fangming et. al. [36] experimental study was used for alloy type and molten temperature to find viscosity, density and surface tension. Methods used to find

density, viscosity and surface tension were elaborated in the theoretical section of this study.

Table 12: Similarities between foaming process in molten Al-Si and Water-ethanol.

Property	aqueous foam	metal foam
viscosity	1.44	1.3
Density	0.983	1.02
Surface tension	0.68	0.92
volume fraction	15%	7%

5. Conclusion.

5.1. Best foaming condition.

The first part results showed that, best foaming condition for water ethanol mixture occurred at 0.15 ethanol volumetric fraction. This value is specified depending on two factors collapse time and number of bubbles. While, for isopropyl foam did not appear.

This result can be justified according to Schutz [15] experimental study. In his investigation he used shaking of a closed tube containing foaming mixture. For water ethanol mixture, most stable foam occurred at 0.15 ethanol volume fraction. While for water isopropyl mixture, foam occurred at two volume fractions: The first one is at 0.005 volume fraction with good collapse time of 18 seconds. The second fraction is at 0.3 volume fraction with a very unstable foam which have collapse time of 3.6 seconds. Also, he ignored the isopropyl foaming at 0.005 volume fraction due to very low concentration, which means that maybe isopropyl is not the main reason of foaming and foaming occurred because of impurities.

In conclusion, there are two main reasons why foam did not appear for isopropyl in this study:

- Used method: air injection with open mixture storage. While in Schutz work, he used shaking of closed tube method which create more stable foam.
- Traube's rule: surface activity is strongly related to the length of hydrocarbon chain. So that, as isopropyl has one more carbon atom than ethanol this leads to higher surface activity and lower surface tension. That is why longer chains of alcohol are considered defoaming agents.

5.2. Effect of flow rate and foaming time on diameter and number of bubbles.

According to figure (13) Foaming time does not have a significant impact on diameter. While, flow rate has a proportional effect on diameter. Except for point (50L/h and 55 seconds) a significant drop in diameter happened due to the small available storage area which lead to the bubbles to overcrowd and destroy each other into smaller ones. Also, mean diameters at 75 L/h were small for same reason.

According to figure (12) foaming time has a proportional impact on bubbles number. While, the flow rate does not have a significant impact. And the irregularities for point (50L/h and 55 seconds) and flow rate of 75 L/h caused because of bubbles overcrowding.

In conclusion, significant relations are illustrated below:

- Bubbles number can be controlled by foaming time.
- Diameter can be controlled by flow rate.
- Foam stability can be predicted by alcohol molecular structure, mixture viscosity and surface tension.

5.3. Drainage velocity and dimensionless numbers.

The drainage rate was calculated with simple way: liquid content within foam over collapse time. Liquid content was very low and could not be detected by eye so approximated values were used. Because neither approximations nor actual values, will affect velocity or dimensionless numbers significantly.

In conclusion, according to the proposed relation for drainage velocity. Drainage velocity is mainly dependent on foam thickness and collapse time. While the liquid content volume did not have a significant impact in case of dry foam.

5.4. Similarities between foaming process in water alcoholic mixture and Al-Si alloy.

Foaming process stability in aqueous solution depends mainly on the surfactant volume fraction. While for molten metal stability is controlled by size, concentration, type, and surface tension of solid particles. Therefore, investigation on alloying element was used in this study. Because it is not possible to use solid particles for aqueous foam as they will act as a defoaming agent.

5.5. Magnetic field effect.

The effect of magnetic field could not be investigated. Because salt addition has a significant negative impact on foam stability. And this effect is in agree with Varade et. al. [31] study, at which they proved experimentally that salt has negative impact as well. To investigate magnetic field effect, it is advised to use much stable foam (since foam from alcohol solution are considered relatively unstable).

Bibliography

- [1] I. H. S. K. Iljoon Jin, Kingston; Lorne D. Kenny, "United States Patent-METHOD OF PRODUCING LIGHTWEIGHT FOAMED METAL," vol. 96, no. 19, pp. 62–66, 1990.
- [2] O. Prakash, H. Sang, and J. D. Embury, "Structure and properties of AlSiC foam," *Mater. Sci. Eng. A*, vol. 199, no. 2, pp. 195–203, 1995.
- [3] S. W. Ip, Y. Wang, and J. M. Toguri, "Aluminum foam stabilization by solid particles," *Can. Metall. Q.*, vol. 38, no. 1, pp. 81–92, 1999.
- [4] W. Deqing and S. Ziyuan, "Effect of ceramic particles on cell size and wall thickness of aluminum foam," *Mater. Sci. Eng. A*, vol. 361, no. 1–2, pp. 45–49, 2003.
- [5] A. R. Kennedy and S. Asavavisithchai, "Effect of ceramic particle additions on foam expansion and stability in compacted Al-TiH₂ powder precursors," *Adv. Eng. Mater.*, vol. 6, no. 6, pp. 400–402, 2004.
- [6] T. Iida, "Physical properties of liquid metals [IV] surface tension and electronic transport properties of liquid metals," *Weld. Int.*, vol. 8, no. 10, pp. 766–770, 1994.
- [7] R. Takaki, "Surface tension measurement of high temperature metallic melt.," *Tech. Rep. Natl. Aerosp. Lab.*, vol. 1407, pp. 1–18, 2000.
- [8] X. J. Han, M. Chen, and Z. Y. Guo, "A molecular dynamics study for the thermophysical properties of liquid Ti-Al alloys," *Int. J. Thermophys.*, vol. 26, no. 3, pp. 869–880, 2005.
- [9] H. Eyring, "Physical Chemistry: An Introduction (Moelwyn-Hughes, E. A.)," *J. Chem. Educ.*, vol. 18, no. 6, p. 300, Jun. 1941.
- [10] F. D. Richardson, *Physical chemistry of melts in metallurgy*, vol. 1.

Academic press, 1974.

- [11] C. Marangoni, "Marangoni," *C. Nuovo Cim.*, vol. [2] 5-6' 2, 1878.
- [12] "Joseph Plateau-Statique experimentale et theorique des liquides soumis aux seules forces moleculaires ~ French and English versions." .
- [13] K. L. G. Kretzschmar, *physical chemistry*. 1970.
- [14] "Elasticity of Thin Liquid Films * frame __ ~ J ~ odium r Twater jacket," vol. 0, pp. 1-7, 1967.
- [15] F. SCHUTZ, "E X P E R I M E N T S ON FOAM TIME . PART 11 . E X P E R I M E N T S WITH A L I P H A T I C ALCOHOLS AND A RELATION B E T W E E N CHAIN LENGTH AND FOAM TIME . CRITICAL," 1942.
- [16] P. R. Garrett, "Defoaming: Antifoams and mechanical methods," *Curr. Opin. Colloid Interface Sci.*, vol. 20, no. 2, pp. 81-91, 2015.
- [17] S. I. Karakashev and M. V. Grozdanova, "Foams and antifoams," *Adv. Colloid Interface Sci.*, vol. 176-177, pp. 1-17, 2012.
- [18] N. D. Denkov, K. G. Marinova, and S. S. Tcholakova, "Mechanistic understanding of the modes of action of foam control agents," *Adv. Colloid Interface Sci.*, vol. 206, pp. 57-67, 2014.
- [19] C. Hill and J. Eastoe, "Foams: From nature to industry," *Adv. Colloid Interface Sci.*, vol. 247, no. October 2016, pp. 496-513, 2017.
- [20] I. S. Khattab, F. Bandarkar, M. A. A. Fakhree, and A. Jouyban, "Density, viscosity, and surface tension of water+ethanol mixtures from 293 to 323K," *Korean J. Chem. Eng.*, vol. 29, no. 6, pp. 812-817, 2012.
- [21] F. M. Pang, C. E. Seng, T. T. Teng, and M. H. Ibrahim, "Densities and

- viscosities of aqueous solutions of 1-propanol and 2-propanol at temperatures from 293.15 K to 333.15 K,” *J. Mol. Liq.*, vol. 136, no. 1–2, pp. 71–78, 2007.
- [22] G. Vazquez, E. Alvarez, and J. M. Navaza, “Surface Tension of Alcohol + Water from 20 to 50 °C,” *J. Chem. Eng. Data*, vol. 40, no. 3, pp. 611–614, 1995.
- [23] J. Schmitz, B. Hallstedt, J. Brillo, I. Egry, and M. Schick, “Density and thermal expansion of liquid Al-Si alloys,” *J. Mater. Sci.*, vol. 47, no. 8, pp. 3706–3712, 2012.
- [24] H. Kobatake, J. Brillo, J. Schmitz, and P. Y. Pichon, “Surface tension of binary Al–Si liquid alloys,” *J. Mater. Sci.*, vol. 50, no. 9, pp. 3351–3360, 2015.
- [25] G. B. Stringfellow and C. Hewlett-Packard Co., Palo Alto, “THE CALCULATION OF REGULAR SOLUTION INTERACTION PARAMETERS BETWEEN ELEMENTS FROM GROUPS III, IV AND V OF THE PERIODIC TABLE*,” vol. 6, pp. 639–640, 1971.
- [26] Z. Pang and H. Liu, “The study on permeability reduction during steam injection in unconsolidated porous media,” *J. Pet. Sci. Eng.*, vol. 106, pp. 77–84, 2013.
- [27] J. Banhart, “Manufacturing Routes for Metallic Foams,” *Jom*, vol. 52, no. December, pp. 22–27, 2000.
- [28] H. Kister, “Distillation Operation.” p. 729, 1990.
- [29] R. H. Perry and D. W. Green, *Chemical Engineers’ Handbook*. 1997.
- [30] C. J. W. Breward and P. D. Howell, “The drainage of a foam lamella,” *J. Fluid Mech.*, vol. 458, pp. 379–406, 2002.

- [31] S. R. Varade and P. Ghosh, "Foaming in aqueous solutions of zwitterionic surfactant: Effects of oil and salts," *J. Dispers. Sci. Technol.*, vol. 38, no. 12, pp. 1770–1784, 2017.
- [32] j.j. bikerman, *foams*, vol. 112, no. 483. 1966.
- [33] P. Stevenson, "Dimensional analysis of foam drainage," *Chem. Eng. Sci.*, vol. 61, no. 14, pp. 4503–4510, 2006.
- [34] S. J. Neethling and J. J. Cilliers, "The physical modeling of foam and froth behavior," *Chem. Eng. Technol.*, vol. 24, no. 12, pp. 1309–1312, 2001.
- [35] A. Asbeck, P. E. R. Padgett, F. Application, and P. Data, "United States Patent (19)," vol. 180, no. 19, pp. 3–8, 1978.
- [36] X. Fangming, W. Qian, X. Qingyan, and X. Shoumei, "Preparation of aluminum foam by gas injection foaming," *Spec. Cast. Nonferrous Alloy.*, vol. 27, no. 7, pp. 563–565, 2007.

Annex 1: Image Processing Code.

➤ Input part:

```
Image = 'insert image name:';
Image = input(Image,'s');
Scale = 'insert Scale (pixels/mm)';
Scale = input(Scale);
contrast = 'insert additional required contrast (0-255): ';
contrast = input(contrast);
Text2 = 'insert morphological function (0,1 and 2 for non,
erode and opening):';
Text2 = input(Text2);
if Text2 == 1 || Text2 == 2
    se = 'insert disk structural element size (1-5):';
    se = input(se); % for morphological function.
end
Noise = 'insert noise reduction value:';
Noise = input(Noise); %any particle less than noise-pixel will
be deleted
Noise = Noise;
Circl = 'choose circularity:';
Circl = input(Circl);
low_size = 'insert smallest diameter you want in mm:';
low_size = input(low_size);
max_size = 'insert largest diameter you want in mm:';
max_size = input(max_size);
```

➤ Preprocessing part:

```
ar = imread(Image);
a = rgb2gray(ar); % switch image to gray scale
a1 = adapthisteq(a); % Contrast1.
a2 = imhmax(a1,contrast); % Contrast2.
a3 = imbinarize(a2,graythresh(a2)); % threshold.
a4 = imcomplement(a3); % switch between B&W.
a5 = imclearborder(a4);
a5 = imfill(a5, 'holes' ); % fill holes
```

```

if Text2 == 1
    a6 = imerode(a5, strel('disk',se,8)); % erode.
else
    if Text2 == 2
        a6 = imopen(a5, strel('disk',se,8)); % open.
    else
        if Text2 == 0
            a6 = a5;
        end
    end
end
end
a7 = bwareaopen(a6, Noise); % noise reduction
a8 = imclearborder(a7);
boundaries = bwperim(a8);
Pre_processed = bwconvhull(Pre_processed, 'objects', 8);
figure, imshow(ar), title('real image')
figure, imshow(a1), title('Contrast')
figure, imshow(a2), title('Additional Contrast')
figure, imshow(a3), title('Threshloding')
figure, imshow(a4), title('Switch between B&W')
figure, imshow(a5), title('border cleaning and filling')
figure, imshow(a6), title('Effect of Morphological function')
figure, imshow(a7), title('Noise Reduction')
figure, imshow(a8), title('Boarder Cleaning')
figure, imshow(boundaries), title('Objects Outlines')
figure, imshow(Pre_processed), title('final pre-processed
image')

```

➤ Processing part:

Detecting objects (bubbles):

```

cc = bwconncomp(Pre_processed,4);
data = regionprops(cc, 'Area', 'Centroid', 'BoundingBox',
'Circularity', 'EquivDiameter', 'PixelIdxList');
Area = [data.Area] / Scale^2;
Circularity = [data.Circularity];

```

```
EquivDiameter = [data.EquivDiameter] / Scale;
```

Computing required areas and Circularities:

```
LL = (Circularity(1:size(Area,2)) > Circl &  
EquivDiameter(1:size(Area,2)) > low_size &  
EquivDiameter(1:size(Area,2)) < max_size); % logical locations  
Area_Req = Area(LL); % returns required area matrix.  
Circularity_Req = Circularity(LL); % returns required  
Circularity matrix.  
EquivDiameter_Req = EquivDiameter(LL); % returns required  
diameter matrix.  
area_squaredmm = [mean(Area_Req) ; max(Area_Req) ;  
min(Area_Req)]; % area criticals.  
diameter_mm = [mean(EquivDiameter_Req) ; max(EquivDiameter_Req)  
; min(EquivDiameter_Req)]; % diameter criticals.  
circularity = [mean(Circularity_Req) ; max(Circularity_Req) ;  
min(Circularity_Req)]; % circularity criticals.  
Number = [size(Area_Req,2);size(Area_Req,2);1]; % number of  
objects  
  
LN = find(Circularity(1:size(Area,2)) > Circl &  
EquivDiameter(1:size(Area,2)) > low_size &  
EquivDiameter(1:size(Area,2)) < max_size); % returns locations  
number in area matrix.  
C_Objects = false(size(Pre_processed));  
for i = LN  
    C_Objects(cc.PixelIdxList{i}) = true;  
end  
Unc_Objects = Pre_processed - C_Objects;  
  
% Coloring counted objects:  
labeled = bwlabel(C_Objects);  
labeled = label2rgb(labeled,'spring','c','shuffle');
```

Creating output area table:

```
Area_Array = transpose (Area_Req);
Area_Table =
array2table (Area_Array, 'VariableNames', {'Area_squaredmm'});
Count_Array = transpose ( 1:size (Area_Req,2));
Count_Table =
array2table (Count_Array, 'VariableNames', {'Count'});
Circularity_Array = transpose (Circularity_Req);
Circularity_Table =
array2table (Circularity_Array, 'VariableNames', {'Circularity'});
EquivDiameter_Array = transpose (EquivDiameter_Req );
EquivDiameter_Table =
array2table (EquivDiameter_Array, 'VariableNames', {'Diameter_mm' }
);

Name = {'mean'; 'max' ;'min'};
Avg_table = table (Name, Number, area_squaredmm , diameter_mm ,
circularity);
```

Results:

```
figure, imshow (C_Objects), title ('Counted Objects')
figure, imshow (Unc_Objects), title ('Uncounted Objects')
figure, histogram (EquivDiameter_Req), title ('Diameter
Histogram')
figure, histogram (Circularity_Req) , title ('Circularity
Histogram')
figure, imshow (labeled), title ('Colored Counted Objects')
uitable (uifigure, 'data' , [Count_Table, Area_Table,
EquivDiameter_Table, Circularity_Table])
uitable (uifigure, 'data' , [Avg_table])
```